81P ALTERATIONS IN ADHESION MOLECULE EXPRESSION ON RABBIT BALLOON INJURED SUBCLAVIAN ARTERIES: MODULATION OF LEUKOCYTE ADHESION

S. Kennedy, [1]A.R.McPhaden, R.M. Wadsworth & C.L. Wainwright Dept. of Physiology and Pharmacology, University of Strathclyde, Glasgow, G1 1XW and [1]Dept. of Pathology, Glasgow Royal Infirmary, Glasgow.

There is a substantial body of evidence to implicate leukocytes in both the immediate and the long-term effects of vascular injury induced by balloon angioplasty. Following injury, activated leukocytes rapidly adhere to damaged endothelium and migrate into the vessel wall (Pärsson *et al* 1994) and this may ultimately contribute to the development of neointima (Golino *et al* 1997). The adhesion of leukocytes to vessel walls requires interaction between vascular and leukocyte adhesion molecules and recently it has been demonstrated that balloon angioplasty can induce changes in vascular adhesion molecules (Kurz *et al* 1994). In a previous study we have show that leukocyte adhesion to balloon injured rabbit subclavian arteries is enhanced 24 and 48 hours after injury (Kennedy *et al* 1997) and in the present study we have examined adhesion molecule expression on normal and injured vessels in an attempt to discover the cause of enhanced leukocyte adhesion after vascular injury.

Normal rabbits and rabbits which had been fed a cholesterol-supplemented diet for 4 weeks prior to angioplasty were studied. Angioplasty of the left subclavian artery was performed under halothane/nirous oxide anaethesia (Hadoke *et al* 1995) and rabbits were euthanised 2 hours, 24 hours, 48 hours or 8 days later. All cholesterol-fed animals were euthanised 24 hours after angioplasty. Left and right subclavian arteries were removed, fixed in neutral buffered formalin, embedded in paraffin and cut into 4μm sections. One section from each artery was stained with haematoxylin and eosin and three slides were used for immunocytochemical (ICC) studies. Three antibodies were studied: ICAM-1, E-selectin and VCAM-1. All three were incubated overnight, at dilutions of 1/500 (ICAM-1) or 1/1000 (E-selectin, VCAM-1). Antibody was conjugated with biotinylated secondary antibody and detected using peroxidase-labelled streptavidin and diaminobenzidine. Morphological characteristics were graded on a three-point scale and antibody staining on a five-point scale by an investigator blinded to status of the vessel.

Non-injured right subclavian arteries had no visible damage and an intact endothelium. Control arteries from hypercholesterolaemic animals showed no evidence of atheroma although some degree of endothelial dysfunction was apparent in functional experiments. Injured arteries had a variable degree of damage which tended to decrease from the vessel lumen to the adventitia. Some vessels had necrotic areas of smooth muscle in the media which were associated with extensive inflammatory cell influx. Two vessels removed after 8 days had visible neointimal growth.

ICC studies revealed increased levels of E-selectin and VCAM-1 24 and 48 hours after balloon angioplasty which reached significance at the 48 hour time point (staining grade was 1.5±0.2 in the injured artery vs. 0.9±0.1 in the control artery for E-selectin at 48 hours, n=7; $p<0.05$ and 1.2±0.2 vs. 0.5±0 for VCAM-1 at the same time point, n=7; $p<0.05$). No change was found in the level of ICAM-1 staining at any time point. Hypercholesterolaemia did not induce any significant alteration in the expression of any of the three adhesion molecules on control or injured arteries compared to normocholesterolaemic arteries removed 24 hours after injury.

This study has demonstrated that leukocyte accumulation in the media of rabbit subclavian arteries occurs after balloon-induced injury. Furthermore, the enhanced leukocyte adhesion which is observed in this model 24 and 48 hours after arterial injury may be related to increased expression of adhesion molecules on the injured vessel.

Golino, P., Ambrosio, G., Ragni, M. (1997) *Thromb. Haemost.* 77(4): 783-788.
Hadoke, P.W.F., Wadsworth, R.M., Wainwright, C.L. (1995) *Coron. Artery Dis.* 6: 403-415.
Kennedy, S., Wainwright, C.L., Wadsworth, R.M. (1997) *J. Mol. Cell. Cardiol.* 29(5): Sa82 (abstr.).
Kurz, R.W., Graf, B., Gremmel, F. (1994) *Clin. Sci.* 87: 627-633.
Pärsson, H., Cwikiel, W., Johansson, K., (1994) *Cardiovasc. Intervent. Radiol.* 17: 190-196.

82P EFFECTS OF ATROPINE ON THE BRADYCARDIA ASSOCIATED WITH PRIMARY THORACIC BLAST INJURY IN THE ANAESTHETIZED RAT

M. Ohnishi, E. Kirkman & *P. Watkins, Department of Biological Sciences, Science Laboratories, University of Durham, Durham DH1 3LE & *DERA, Medical Countermeasures, CBD, Porton Down, Salisbury, SP4 0JQ

Primary blast injury to the thorax induces a bradycardia, hypotension and apnoea (Krohn *et al.*, 1942). This triad of changes appear to be reflex in nature with vagal afferent and/or efferent pathways. Previous work has shown that the bradycardia and apnoea can be abolished completely and the hypotension attenuated by vagotomy (Ohnishi *et al.*, 1997). The aim of the current study was to determine whether the bradycardia is mediated by an increase in vagal efferent activity, and hence can be prevented with atropine.

Experiments were performed on 4 groups of male Wistar rats (246-266 g body weight) anaesthetized with alphadolone/ alphaxalone (19-21 $mg.kg^{-1}.h^{-1}$ iv). Heart period (HP) was measured from the electrocardiogram recorded via needle electrodes attached to the skin, blood pressure via a cannula inserted into the ventral tail artery and body temperature via a rectal probe. Body temperature was maintained constant at 38.0±0.0 °C (mean±s.e.mean) using external heating.

Group I (n=9) and IV (n=5) received 0.9% saline (1 $ml.kg^{-1}$ iv) while Groups II (n=8) and III (n=8) received atropine sulphate (0.3 $mg.kg^{-1}$ iv). 10-15 min later baseline measurements were made and the animals subjected to a blast wave focused on the ventral thorax (Groups I and II, Tatic *et al.*, 1996), or the sound of blast (Groups III and IV, sham blast). In Group I HP increased significantly from 128±2 ms at baseline to 433±35 ms after blast ($P<0.05$, repeated measures analysis of variance, latency 4.7±0.4 s), and was still elevated 30 min after blast when HP was 160±5 ms. Mean arterial blood pressure (MBP) fell significantly from 124±3 mmHg at baseline to 36±2 mmHg after blast (latency 2.1±0.1 s) and 92±5 mmHg 30 min later. In Group II blast produced a significant increase in HP above baseline (HP 124±3, 142±3 and 142±4 ms at baseline, after blast and 30 min later, respectively). However, the blast-induced increase in HP seen in Group II was far less than that seen in Group I. MBP fell significantly in Group II from a baseline of 126±4 mmHg to 45±4 mmHg after blast and 91±4 mmHg 30 min later. Sham blast did not produce any cardiovascular effects in Groups III or IV.

These results indicate that most of the bradycardia induced by thoracic blast can be abolished by atropine, suggesting that it is largely due to activation of vagal efferent fibres to the heart. Atropine, however, does not modify the blast-induced hypotension.

This work was supported by DERA, Porton Down.

Krohn, P. L., Whitteridge, D., & Zuckerman, S. (1942). Lancet (i), 252-258.

Ohnishi, M., Kirkman, E. & Guy, R. (1997). Journal of Accident and Emergency Medicine, *in press*.

Tatic, V. *et al.*, (1996). Journal of Trauma 40, S94-S99.

83P GENERATION AND CHARACTERISATION OF MURINE MACROPHAGE CELL LINES TRANSFECTED WITH SENSE AND ANTISENSE LIPOCORTIN-1 (LC-1) cDNA

H.J. Harris, S.D. Keating*, R. J. Flower*, R. Hannon* and C.E. Bryant
*Department of Clinical Veterinary Medicine, The University of Cambridge, Madingley Road, Cambridge, CB3 OES, UK.*Department of Biochemical Pharmacology, St Bartholomew's and the Royal London School of Medicine, London, EC1M 6BQ*

Lipocortin-1 (LC-1) suppresses the expression of inducible nitric oxide synthase (iNOS) in response to lipopolysaccharide (LPS) in murine macrophages (Wu *et al.*, 1995). To determine the mechanisms involved in LC-1 suppression of iNOS, we have stably transfected a murine macrophage cell line (RAW 264) with sense and antisense LC-1 cDNA. Here we report the resultant LC-1 levels and differences in morphology between the cell types.

LC-1 cDNA was amplified from murine RNA using rt-PCR. The LC-1 fragment was subcloned into the pCRTII vector (Promega) for sequence confirmation and then cloned into the pRc/RSV eukaryotic expression vector (Invitrogen) in a sense (forward; F) or antisense (reverse; R) orientation. For transfection, RAW cells were grown in DMEM containing 10 % FCS supplemented with glutamine (2 mM), penicillin (200 U/ml) and streptomycin (100 µg/ml). Cells received 5 µg of control vector (C; pRc/RSV with no insert), F-vector or R-vector, together with 10 µl Lipofectin (Gibco) in serum-free medium for 24 h. Complete medium was added after 24 h. Selection of transfected cells was performed after 48 h using G418 (500 µg/ml). Antibiotic-resistant cells were grown to confluency. For characterisation, cell-surface LC-1 was removed by an EDTA (1 mM) wash containing protease inhibitors (E-wash), and intracellular LC-1 removed by an EDTA (10 mM)/ triton X100(1 %)/ protease inhibitor wash. LC-1 protein was measured by western blot analysis. Sheep anti-human LC-1 antibody was used at 1:50,000 and protein bands visualised by enhanced chemiluminescence (Amersham). Cell lines were selected that over- (F) or under-expressed (R) LC-1.

F, R, C and untransfected RAW cells were plated at equal density ($2x10^4$/ml) onto 6 well plates for 48 h. After 24 h at confluency, cellular morphology was assessed by light microscopy and viable cells were counted using trypan blue exclusion (mean data expressed as million cells/ml±sem). The remaining cells were washed with E-wash and coated onto 96 well plates for ELISA using sheep anti-human LC-1 antibody (1:4000) and readings taken at OD 490 nm.

Of the cell lines showing G418 resistance (C: n=7; F: n=32; R: n=10), three F cell lines generated more LC-1 and three R cell lines produced less LC-1 compared to C cells, which all exhibited equal levels of LC-1. One cell line from each group demonstrating the most pronounced over- or under- expression of LC-1 respectively was selected by western blot analysis for the characterisation studies. Cellular morphology differed between the cell types. R cells showed a large number of membrane projections, C and untransfected RAW cells had less projections and F cells were completely rounded. All cell types remained adherent to the culture dish and basal cellular proliferation did not differ between the cell types (C: 1.8±0.4; F: 1.2±0.1; R: 1.8±0.5 million cells/ml; n=3). ELISA was used to quantify changes in LC-1 protein expression. Basal extracellular LC-1 levels tended to be higher in the F cells (133%±13; (P=0.06, ANOVA, n=3) compared to C (100 %) or R cells (104%±5).

We have generated three cell populations that express different amounts of basal LC-1 and these chronic changes are associated with differing morphology between transfected RAW cell types.

This work was supported by the Wellcome Trust.

Wu, C.C., *et al.*, 1995, Proc. Natl. Acad. Sci. **92**, 3473-3477

84P THE EFFECT OF CHRONIC OVER-EXPREESSION OF LIPOCORTIN-1 (LC-1) ON THE CELLULAR RESPONSES TO LIPOPOLYSACCHARIDE (LPS)

H.J. Harris, R. Hannon* & C.E. Bryant
*Department of Clinical Veterinary Medicine, The University of Cambridge, Madingley Road, Cambridge, CB3 OES, UK. *Department of Biochemical Pharmacology, St Bartholomew's and the Royal London School of Medicine, London, EC1M 6BQ*

We have previously shown that acute treatment with lipocortin-1 (LC-1) neutralising antibody reverses the suppression of inducible nitric oxide synthase (iNOS) caused by dexamethasone treatment in lipopolysaccharide (LPS)-treated rats *in vivo* (Wu *et al.*, 1995), suggesting a role for LC-1 in regulating iNOS. Here, we have used stably transfected murine macrophage cell lines (RAW 264) with sense and antisense LC-1 genes (Harris *et al.*, this meeting) to study the responses of these cells to LPS.

Control (transfected with vector alone) (C), sense (F), antisense (R) and untransfected (RAW) cells were plated at equal density ($2.5x10^4$/ml) onto 96 well plates for 48 h in DMEM supplemented with glutamine (2 mM), penicillin (200 U/ml), streptomycin (100 µg/ml), FCS (10 %) and G418 (500 µg/ml). At ~80% confluency, cells were treated with LPS (0.1-10 µg/ml) or vehicle for 24 h. Viable cell proliferation was assayed using the Cell Titre 96™ Non-Radioactive Cell Proliferation Assay (Promega) and cell number expressed as optical density (OD) units at 550-630 nm. NOS activity was measured by nitrite accumulation (NO^{2-} µM) in the medium using the Griess reaction and normalised for cell number, relative to C cells. In addition, electrophoretic mobility shift assays (EMSA) for measurement of activated nuclear factor kappa beta (NfKβ; Gel Shift Assay System; Promega) were performed on nuclear pellets prepared from confluent 6 well plates treated with LPS (1 µg/ml) for 0.5-6h.

Basal cell proliferation did not vary between transfected cells, or compared to untransfected cells. However, LPS (1 µg/ml) significantly reduced cell numbers compared to vehicle in F and R cells, but not in C or RAW cells (2-sample t-test, *P<0.05, n=3-4; see table; mean OD units±sem).

	C	F	R	RAW
-LPS	1.28±0.08	1.27±0.07	1.26±0.07	1.31±0.05
+LPS	1.08±0.08	0.94±0.06*	1.00±0.04*	1.09±0.08

Suprisingly, F cells over-expressing LC-1 produced significantly more NO^{2-} /million cells (287%±89) in response to LPS (1 µg/ml, P<0.01; ANOVA, n=5) when compared to C (100 %), R (101%±41) or RAW (158%±62) cell lines.

LPS (1 µg/ml) caused activation and nuclear translocation of NfKβ in all cell types (n=4). However, the time course of NfKβ nuclear translocation differed. C and F cells showed NfKβ nuclear translocation between 0.5-4 h whereas R cells exhibited sustained nuclear NfKβ presence up to 6 h after LPS stimulation.

Here we show that chronic elevation of LC-1 levels in over-expressing F cells enhances LPS-induced NO production. C, R and RAW cells produce similar amounts of NO in response to LPS. All cell types show nuclear translocation of NfKβ in response to LPS, but, interestingly, a reduction in LC-1 levels in R cells is associated with prolonged nuclear translocation of NfKβ. As the iNOS promoter contains NfKβ consensus sites (Xie *et al.*, 1994) and NfKβ activation was unchanged between C and F cells, it is possible that chronic elevation of LC-1 levels may activate additional signalling pathways to produce iNOS in F cells.

This work was supported by the Wellcome Trust.

Wu, C.C., *et al.*, 1995, Proc. Natl. Acad. Sci. **92**, 3473-3477
Xie, Q., Kashiwabara, Y. and Nathan, C., 1994 J. Biol. Chem. **269**, 4705-4708

85P INTERLEUKIN-1 MODIFIES EXCITOTOXIC CELL DEATH INDEPENDENTLY OF EFFECTS ON BODY TEMPERATURE

R.I.Grundy, N.J.Rothwell, & S.M.Allan, School of Biological Sciences, University of Manchester, 1.124 Stopford Building, Oxford Road, Manchester M13 9PT, UK.

The cytokine, interleukin-1 (IL-1) has diverse actions in the brain, which include marked effects on body temperature. IL-1 has also been implicated in neurodegeneration (Rothwell and Hopkins, 1995). It is well established that hyperthermia aggravates ischaemic brain injury (Busto et al., 1987). We investigated the link between the febrile responses to IL-1 and its effects on neurodegeneration.

Male, Sprague-Dawley rats (250-325g) were anaesthetised with halothane, and injected into the striatum (co-ordinates from Bregma: AP +0.7 mm, ML -2.7 mm, and DV -5.5 mm), hypothalamus (co-ordinates from Bregma: AP –0.4 mm, ML – 0.6 mm, and DV –8.0 mm) or cerebral ventricles (ICV) with 1μl recombinant human IL-1β (10 ng), immediately followed by striatal injection of 1μl of the excitotoxin S-AMPA (7.5 nmol). Body temperature was then monitored at 10 minute intervals using remote radio telemetry via abdominally implanted transmitters. Animals were sacrificed 48 hours after infusion brains removed, frozen, and cut (20μm sections) every 250μm throughout the lesion. Sections were then stained with cresyl violet for the histological analysis of neural damage. Data were analysed using either ANOVA for differences between more than two groups, or Student's t-test for differences between two groups.

Basal temperatures of all animals ranged from 36.9-37.2 °C. The peak temperature response to striatal injection of S-AMPA (38.0 ± 0.1°C; n=6) was not significantly different to that of striatal co-injection of IL-1 and S-AMPA (38.9 ± 0.3°C; n=4). S-AMPA infused in the striatum resulted in widespread cell death throughout this region (lesion volume = 25.9 ± 2.2mm^3), with slight damage in the overlying cortex. Striatal co-infusion of S-AMPA and IL-1 produced both local (striatal) and significant cortical damage (102.0 ± 19.3mm^3) ($P<0.05$). The maximal temperature response to injection of IL-1 (ICV) and striatal S-AMPA (38.9 ± 0.2°C; n=9) was significantly greater than S-AMPA alone in the striatum (37.5 ± 0.4°C; n=8) ($P<0.05$). No cortical damage was seen when IL-1 was injected ICV in spite of the marked febrile response. IL-1 (hypothalamus) and S-AMPA (striatum) produced a peak temperature (38.8 ± 0.4°C; n=5) that was not significantly different to S-AMPA alone in the striatum (38.2 ± 0.3°C; n=4). Cortical damage was also seen in 50% of animals treated with striatal S-AMPA and hypothalamic IL-1.

Thus, although IL-1 injected into the striatum or the hypothalamus causes fever and exacerbation of damage, injection ICV induces marked fever but no increase in damage. These observations suggest that increases in body temperature in response to IL-1 cannot, alone, be responsible for its effects on neuronal damage.

This work was supported by MRC.

Rothwell, N.J. & Hopkins, S.J. (1995) *TINS* 18, 130-136.
Busto, R. Deitrich, W.D., Globus, M.Y.-T. *et al.* (1987) J.Cereb.Blood Flow Metab. 7, 729-738.

86P BRAIN SITES OF ACTION OF INTERLEUKIN-1 IN FEVER

T. Cartmell & N.J Rothwell, School of Biological Sciences, 1.124 Stopford Building, University of Manchester, Manchester M13 9PT.

Interleukin (IL)-1 is a potent endogenous pyrogen which acts directly on the CNS to induce fever. Interleukin-1 receptor antagonist (IL-1ra), a naturally occuring protein that binds to IL-1 receptors, inhibits endotoxin fever in the rat when injected into the cerebral ventricles. Ventricular administration, however, often results in diffusion of substances throughout the brain and does not reveal the primary sites of action. Recent findings support a direct involvement of IL-1 and IL-1ra in acute and chronic cerebral neuropathologies and suggest that these molecules have highly specific sites of action, probably in the striatum (Rothwell, 1997). We therefore investigated the effects of IL-1ra injected into discrete brain sites on core body temperature and fever.

Male, Sprague-Dawley rats (250-350g) were stereotaxically implanted (at least 7d prior to experimentation) with indwelling guide cannulae (under halothane anaesthesia) into the lateral cerebral ventricle (i.c.v), anterior hypothalamic preoptic area (AH/POA), striatum or cortex. Core temperature (peritoneal) was measured by remote radiotelemetry. Sites of action of endogenous brain IL-1 in fever were investigated in unrestrained rats by injecting lipopolysaccharide (LPS; 100μg/kg) into a subcutaneous air pouch (i.p.o.) followed by human recombinant IL-1ra (50μg in 0.5μl), or saline, into a discrete brain region at 0h and 1h. The site of micro-injection was verified histologically at the end of the experiments. Data were analysed using ANOVA for differences between more than two groups, or unpaired Student's *t*-test for differences between two groups.

Injection of LPS i.p.o. induced a rise in body temperature which commenced 1.5h after injection and was maximal at 3h (38.8±0.1°C (mean±s.e.m)), compared with 37.0±0.1°C at 0h, n=6, $P<0.001$). IL-1ra significantly attenuated LPS fever when injected i.c.v. (IL-1ra 37.5±0.1°C; saline 38.8±0.2°C; $P<0.001$, n=8) or into the AH/POA (IL-1ra 37.7±0.2°C; saline 38.8±0.1°C; $P<0.01$, n=6), but had no effect when administered into the striatum (IL-1ra 38.4±0.3°C; saline 38.5±0.1°C; n=6) or cortex (IL-1ra 38.6±0.1°C; saline 38.6±0.1°C; n=6).

These results indicate that endogenous IL-1 acts directly in the region of the AH/POA to mediate fever, in response to systemic LPS. In contrast, administration of IL-1ra into the striatum or cortex does not influence the febrile response to peripheral inflammation. Attenuation of the febrile response by i.c.v. administration of IL-1ra may reflect diffusion of antagonist throughout the brain, in particular to areas of the anterior hypothalamus. Our data suggest site specific actions of the interleukin-1 family in fever which are distinct from those in neurodegeneration.

This work was supported by a Wellcome Trust International Travelling Fellowship.

Rothwell, N.J. (1997) *Br. J. Pharmacol.* 121, 841-847.

87P MURINE MACROPHAGES ARE STIMULATED TO PRODUCE NITRIC OXIDE BY ANTIGEN-BINDING LYMPHOCYTE-DERIVED PROTEIN FACTORS

F.A. Redegeld, B. Heijdra, M.-C. Knippels, J. Garssen & F.P. Nijkamp. Dept. Pharmacology & Pathophysiology, Utrecht Institute for Pharmaceutical Sciences, Utrecht University, P.O. Box 80.082, 3508 TB Utrecht, the Netherlands.

Contact sensitization (CS) with low molecular weight compounds e.g. picryl chloride, 2,4-dinitrofluorobenzene results in rapid production of antigen-binding lymphocyte-derived protein factors (TCF) in spleen and draining lymph nodes, PCl-f and DNFB-f, respectively. These factors are able to sensitize mast cells for activation upon reencounter of antigen. Recently, it was shown that also macrophages can be activated by antigen-binding protein factors (Ferreri et al, 1991) to produce IL-1, IL-6, TNF-α, and PGE_2. Since macrophages are also an important source of nitric oxide (NO), a compound with various biological activities, we have investigated the effects of antigen-binding factors on NO production by murine macrophages.

DNFB-f and PCl-f were isolated using hapten-affinity chromatography from culture supernatant from spleen cells of DNFB or PCl-sensitized mice, as previously described (Garssen et al, 1994). Murine J774 macrophages (ATCC) ($5x10^5$/well) were incubated in 0.5 ml RPMI/10% FCS at 37°C in 5% CO_2. Cells were stimulated by adding LPS (0.1-1 μg/ml), DNFB-f (20 μg/ml) or PCl-f (20 μg/ml) with or without 50 IU/ml of IFN-γ (Redegeld et al, 1997). At 24 h, supernatant was collected for nitrite analysis by a nitric oxide analyzer (Sievers). Protein expression of inducible NO-synthase (iNOS) was analyzed after fractionation of whole cell lysates on SDS-PAGE, electro-blotting to PVDF and probing with an iNOS specific MAb (Affinity Bioreagents).

Incubation with PCl-f and DNFB-f stimulated J774 macrophages to produce NO, as measured by accumulation of nitrite in the supernatant (table 1). Priming of the cells with IFN-γ synergistically enhanced NO production by these factors. The increase of NO production was accompanied by an upregulation of the expression of iNOS. The stimulation of J774 by PCl-f and DNFB-f was not due to contamination by LPS.

Table 1. NO production (nmol/10^6 cells) by J774 macrophages stimulated by antigen-binding protein factors PCl-f and DNFB-f

stimulation	none	IFN-γ (50 U/ml)
control	2.01±0.18	15.2±0.47#
PCl-F	8.23±1.50*	55.1±1.41*#
DNFB-F	28.6±0.74*	76.8±3.91*#
LPS	44.7±0.14*	83.2±2.18#

* significantly different from control; #significantly different from no IFN-γ, p<0.05.

The PCl-f-induced NO production was susceptible to inhibition by specific inhibitors of both protein kinase C (bisindolylmaleimide (2 μg/ml) and polymyxin B sulfate (0.1 μg/ml)) and protein tyrosine kinase (genistein (0-50 μM)), respectively. PKC inhibition completely inhibited NO production. Inhibition of protein tyrosine phosphorylation reduced NO production to 23% of control.

Our data show that macrophages can be activated by TCF to produce increased amounts of NO. Signal transduction pathways involved in the activation by TCF encompass both phosphorylation by PKC and protein tyrosine kinases. TCF play an important role in the initiation of cell-mediated hypersensitivity reactions by priming mast cells for antigen-specific activation, the presented results suggest an addition role for TCF by activation of macrophages. NO can have dual modulatory activities on events involved in CS reactions; by promoting leukocyte accumulation and oedema formation, affecting proliferation and cytokine production by Th1 lymphocytes, and inhibition of mast cell proliferation and stimulation. Therefore, the physiological importance of an increased NO production by TCF-stimulated macrophages warrants further investigation.

Ferreri, N.R., Millet, I., Paliwal, V. *et al*, (1991) *Cell. Immunol.* 137, 389-405
Garssen, J., Van Loveren, H., Kato, K., *et al*, (1994) *J. Immunol.* 153, 32-40 (1994)
Redegeld, F.A., Heijdra, B., Knippels, M.-C. *et al*, (1997) *Immunol. Lett.* 57, 147-149.

88P MEFLOQUINE POTENTIATES HALOFANTRINE-INDUCED QTc PROLONGATION BY ALTERING THE DISTRIBUTION OF HALOFANTRINE

Susan J. Coker, Ian D Lightbown, Dyfrig A Hughes, James P Lambert & Geoffrey Edwards, Department of Pharmacology & Therapeutics, University of Liverpool, Ashton Street, Liverpool L69 3GE.

The antimalarial drug halofantrine can prolong the QT interval of the ECG (Batey *et al.*, 1997) and cause serious arrhythmias such as torsade de pointes. Halofantrine-induced QT prolongation has been reported to be greater in patients who have previously received mefloquine (Nosten *et al.*, 1993).

To investigate possible interactions between these drugs, their effects have been determined in 4 groups (n=6) of pentobarbitone-anaesthetized, ventilated, open chest, female New Zealand White rabbits (2.3 to 3.8 kg) prepared for measurement of arterial blood pressure and limb lead ECG. Increasing doses (1, 3, 10 and 30 mg kg^{-1}) of either halofantrine, mefloquine, halofantrine after 3 mg kg^{-1} mefloquine, or vehicle (dimethyl acetamide 40% / propylene glycol 60% v/v, diluted as required in 5% w/v glucose solution) were given i.v. every 25 min. Arterial blood samples (1ml) were removed 20 min after each dose of drug for determination of halofantrine concentrations by HPLC (Mberu *et al.*, 1992).

Mefloquine up to 10 mg kg^{-1} did not alter ECG intervals, heart rate or blood pressure, but at 30 mg kg^{-1} caused profound reductions in blood pressure, presumably due to cardiac contractile failure. Halofantrine decreased heart rate from 255 ± 15 to 217 ± 15 beats min^{-1} ($P<0.05$, Freidman test) and dose-dependently increased the rate corrected (Bazett's formula) QT interval (QTc) (Table 1a). QTc prolongation by halofantrine was greater in rabbits which had received mefloquine 3 mg kg^{-1}. None of the rabbits had torsade de pointes. Blood concentrations of halofantrine (Table 1b) were approximately twice as high in the group that had received mefloquine, suggesting that mefloquine alters the distribution of halofantrine, perhaps by restricting binding of halofantrine to extravascular sites. This may explain how mefloquine can enhance halofantrine-induced QTc prolongation.

Table 1. The effects of increasing doses of vehicle, halofantrine (HF), mefloquine (MQ), or halofantrine after 3 mg kg^{-1} mefloquine (HF+MQ) on (a) QTc interval and (b) halofantrine concentrations.

a	QTc interval (ms)		
Dose	3 mg kg^{-1}	10 mg kg^{-1}	30 mg kg^{-1}
Vehicle	305±10	311±14	311±11
MQ	307±19	317±17	
HF	361±26	410±19*	410±18**
HF+MQ	439±18*†	452±14*	461±14**†
b	**Halofantrine concentration (μM)**		
Dose	3 mg kg^{-1}	10 mg kg^{-1}	30 mg kg^{-1}
HF	0.7±0.1	3.2±0.3	13.5±1.7
HF+MQ	1.8±0.3†	6.9±1.7†	24.7±4.3†

Values are mean ± s.e. mean. *P<0.05, **P<0.01 compared with vehicle, †P<0.05 compared with HF, Kruskal-Wallis test.

Supported by SmithKline Beecham Pharmaceuticals Ltd.

Batey, A.J., Lightbown, I.D., Lambert, J.P., Edwards, G. & Coker, S.J. (1997). *Br. J. Pharmacol.* 122, 563-569.
Mberu, E.K., Muhia, D.K. & Watkins, W.M. (1992) *J. Chromatogr.* 581, 156-160.
Nosten, F., Ter Kuile, F.O., Luxemberger, C., *et al.*, (1993) *Lancet*, 341, 1054-1056.

89P THE EFFECT OF MIBEFRADIL AND VERAPAMIL ON PERIPHERAL VEINS, COMPARED IN ISOLATED HUMAN SAPHENOUS VEIN PREPARATION

M. Rinia-Feenstra[1,2], B.A.J.M de Mol[2], M. Pfaffendorf[1] & P.A. van Zwieten[1,2].

[1]Department of Pharmacotherapy and [2]Department of Cardiopulmonary Surgery, University of Amsterdam, Academic Medical Centre, Meibergdreef 15, 1105 AZ Amsterdam, The Netherlands.

In the literature the vasodilator effect of verapamil in human saphenous vein (HSV) has been reported in detail. (He et al., 1993). The newer calcium antagonist (CA) mibefradil is an arterial vasodilator, but little is known about its effect on peripheral veins and for this reason we compared the dilator effects of both CA in HSV preparations.

Preparations of HSV were obtained from 10 patients who were subjected to aortocoronary bypass surgery. Prior to the experiments the HSV were stored in University of Wisconsin solution (UW) (Southard et al., 1990) at 4° for a maximum of 2 days. Under these conditions a pilot study showed no significant changes in vasoactive properties. For the experiments rings of endothelium-denuded HSV were mounted into organ baths in oxygenated Krebs solution at 37° at a tension of 4 g., and fixed to an isometric force transducer. Each ring was exposed three times to an isotonic 125 mM KCl solution (KCl), whereafter cumulative concentrations of the CA (1nM to 0.1 mM) were added to the organ bath. Contractions to KCl in the presence of CA were repeated for each concentration of CA and expressed as percentage of the maximal contraction induced by KCl. The data were expressed as mean ± SEM for *n* patients, and significance was analyzed by unpaired, double sided Student's *t* test.

There was no significant difference between absolute values of the maximum contraction to KCl of the verapamil and mibefradil groups of HSV preparations (2.94±0.29 and 2.70±0.23 gram respectively; p=0.5; n=4). In endothelium-denuded HSV preparations verapamil and mibefradil caused concentration-dependent relaxation. Verapamil was a more potent vasodilator compared to mibefradil (pD2 of 5.9±0.04 versus 5.38±0.16 respectively; p<0.05; n=4). Both verapamil and mibefradil did not cause complete relaxation of the potassium-precontracted HSV, but the maximum relaxation differed significantly, 80±1 %relaxation for verapamil versus 52±4%relaxation for mibefradil (p<0.05; n=4).

Comparing the endothelium-independent vasodilator effects of mibefradil and verapamil, the latter appears to be more potent and effective in HSV. Since T-type calcium-channels, which are known to be blocked potently by mibefradil, are completely inactivated under the conditions investigated, the observed differences are likely to be due to particular effects of the two CA on isoforms of the L-type calcium channel or to other compound-specific effects on intracellular homeostasis.

References:
He, G.-W., Rosenfeldt, F.L., Angus, J.A. (1993) *Ann. Thorac. Surg.* 55, pp1210-121 7.
Southard, J.H., Van Gulik, T.M., et al. (1990) *Transplantation* 49, pp251-257.

90P TIME COURSE OF THE RELAXANT ACTION OF VARIOUS CALCIUM ANTAGONISTS IN RAT ISOLATED SMALL MESENTERIC ARTERIES

R. v.d. Lee, M. Pfaffendorf and P.A. van Zwieten, Dept. of Pharmacotherapy, Academic Medical Centre, University of Amsterdam, Meibergdreef 15, 1105 AZ Amsterdam, The Netherlands.

The vasodilator action of calcium antagonists (CA) is known to trigger reflex tachycardia as an undesirable adverse reaction. It is rather the rate of the vasodilator effect than its magnitude which determines the triggering of reflex tachycardia associated with dihydropyridine CA. We therefore compared the rate of the vasodilator effects of a series of CA in rat isolated mesenteric artery preparations. Furthermore we obtained information about the duration of the effect of the CA after the vasodilator-rate protocol by means of the recovery of the response to high-potassium-induced depolarization.

Male Wistar rats (weighing 300-350g.) were anesthetized with ketamine (40 mg i.p.) and xylazine (4 mg i.p.). Small arteries (size 256.2 ± 3.1µm , length 2mm) were dissected from the mesenteric vascular beds and were mounted on an isometric myograph according to Mulvany and Halpern (1977). The individual diameter of each vessel was adjusted to a value that equals 90% of the circumference that a vessel would have at a transmural pressure of 100 mmHg (13.3 kPa). After two initial potassium-induced contractions a third potassium-induced contraction was allowed to be maintained. After 40 minutes one particular concentration of the CA to be studied was administered and the vasodilator effect was measured for maximally 120 minutes. Four concentrations were tested for each CA in separate experiments. Subsequently, the recovery of the response to K^+ was tested by four intermittent K^+-contractions with intervals of 20 minutes. In control experiments (n=6) it was established that a stable response to K^+-induced depolarization could thus be obtained.

The vasodilator effect was quantified by means of IC_{50}-values, and the onset of the effect by the time required to obtain the response associated with the IC_{50}. The mean force of the potasssium-induced contraction amounted to 2.3 ± 0.1mN/mm. The recovery is given as percentages of the fourth potassium-induced contraction in the recovery protocol.

CA studied	IC_{50} ± SEM (nM)	time to IC_{50} ± SEM (min.)	recovery ± SEM (%)
nifedipine	7.2 ± 0.9	7.5 ± 1.1‡	102.2 ± 4.0
mibefradil	34.4 ± 8.3*	22.5 ± 3.6¶	57.2 ± 9.8
barnidipine	0.012 ± 0.002	46.7 ± 6.7	80.4 ± 5.5
(-)-lercanidipine	17.1 ± 3.1†	53.0 ± 9.6	47.5 ± 15.4
(+)-lercanidipine	0.1 ± 0.002	63.3 ± 9.5	23.5 ± 12.7

* means significantly different from all other CA (p<0.01)

† means significantly different from barnidipine and (+)-lercanidipine (p<0.05)

‡ means significantly different from barnidipine and (+)- and (-)-lercanidipine (p<0.05)

¶ means significantly different from (+)- and (-)-lercanidipine

In conclusion, barnidipine and (+)-lercanidipine proved the most potent vasodilator agents. Nifedipine displayed the most rapid onset of action, whereas significantly more time was required to achieve IC_{50}-responses for the other dihydropyridine CA and mibefradil, respectively. Accordingly, nifedipine did not show a prolonged effect after wash-out, whereas the other CA all displayed significantly lower recovery responses, indicating a prolonged effect even after removal of the CA from the medium.

References

1. Mulvany, M.J., Halpern, W. (1977) *Circ. Res.* 41, 19P

91P EVIDENCE THAT AN EARLY DEPRESSION IN MYOCARDIAL CONTRACTILITY CAUSED BY TUMOUR NECROSIS FACTOR-α MAY RESULT FROM THE ACTIVATION OF THE SPHINGOMYELINASE PATHWAY IN THE RAT HEART

N. J. Edmunds and B. Woodward, School of Pharmacy and Pharmacology, University of Bath, Bath, BA2 7AY.

It is well established that the pro-inflammatory cytokine, tumour necrosis factor-α (TNFα), has the potential to decrease myocardial contractility, both *in vivo* and *in vitro*. It is generally accepted that chronic (> 3h) exposure to TNFα decreases contractile function via the induction of nitric oxide synthase. However, an acute (< 20min) negative inotropic effect has also been observed with TNFα, the mechanism of which is less clear. Sphingosine can act as a second messenger in the sphingomyelinase pathway, which is activated by TNFα (Dressler *et al.*, 1992), and has the potential to alter myocardial contractility by disrupting myocyte calcium handling at the level of the ryanodine receptor (Dettbarn *et al.*, 1994).We have observed an early depression in left ventricular contractile function with TNFα and present evidence to suggest the involvement sphingosine in this action.

Hearts from male Wistar rats (280-310g) were perfused, using the Langendorff technique, with recirculating (50ml) Krebs-Henseleit solution (NaCl 118mM, $NaHCO_3$ 25mM, KCl 4.7mM, KH_2PO_4 1.2mM, $MgSO_4$ 1.2mM, CaCl 1.23mM and D-glucose 11.6mM, 95% O_2, 5% CO_2, pH 7.4, 37°C and a flow rate of 10ml/min). Left ventricular developed pressure (LVDP) was measured via an intraventricular balloon. rhTNFα, 20ng/ml, or sphingomyelinase, 0.003U/l were added after 25min. The specific ceramidase inhibitor N-oleoylethanolamine (NOE, 1μM), indomethacin (10μM) or nitro-l-arginine (100μM) were added after an initial 5min stabilisation period.

TNFα caused a negative inotropic effect which was evident within 20min (figure 1), heart rate was not altered (control, 285 ± 11 bpm vs. TNFα, 288 ± 12 bpm, at 90min). This depression in function was blocked by NOE (figure 1). Neither nitro-l-arginine (LVDP, 70 ± 8mmHg, at 90min, n=8) nor indomethacin (LVDP, 66 ± 6mmHg, at 90min, n=6) altered the actions TNFα (LVDP, 83 ± 9mmHg, at 90min, n=10). The negative inotropic affect of sphingomyelinase (LVDP, 34 ± 10mmHg, at 90min, n=7) was also attenuated by NOE (LVDP, 72 ± 10mmHg, at 90min, n=9).

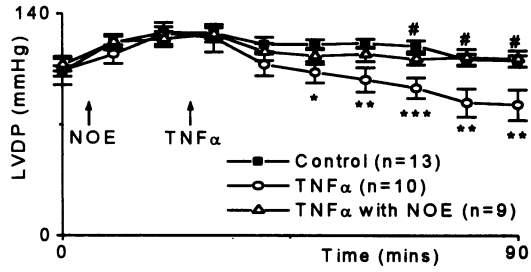

Figure 1. The cardiodepression seen with TNFα can be blocked by NOE. * p<0.05, ** p<0.01, *** p<0.001 TNFα vs. control. # p<0.05 TNFα vs. TNFα and NOE. One way ANOVA coupled to Dunnetts.

These data support the observations of Oral *et al.*, 1997, showing that TNFα causes an early depression in cardiac contractility which is due to activation of the sphingomyelinase pathway. Neither nitric oxide nor prostanoids are appear to be involved in this early depression in cardiac function seen with TNFα.

Sponsored by the British Heart Foundation, FS/94081.

Dattbarn, C.A., Betto, R., Salviati, G., *et al* (1994). *J. Mol. Cell. Cardiol.*, **26**, 229-242.
Dressler, K.A., Mathias, S. and Kolesnick, R.N. (1992) *Science* **255**, 1715-1718.
Oral, H, Dorn, G.W. and Mann, D.L. (1997) *J. Biol. Chem.* **272**, 4836-4842.

92P REDUCED LEVELS OF SMOOTH MUSCLE α-ACTIN mRNA IN RAT MESENTERIC RESISTANCE ARTERIES FOLLOWING SYMPATHECTOMY BUT NOT MYOCARDIAL INFARCTION

F.R.M. Stassen, P.M.E. Lijnen, P.M.H. Schiffers, G.M.J. Janssen, J.F.M. Smits & J.G.R. De Mey. Dept. of Pharmacology and Cardiovascular Research Institute Maastricht, Maastricht University, The Netherlands

Sympathetic nerves have been implicated in maintaining vascular smooth muscle cells (VSMC) in a contractile phenotype. Sympatholytic interventions have been shown to result in the transition from a contractile to a more synthetic phenotype. We evaluated the expression of smooth muscle α-actin (SM α-actin) as a marker of differentiation in mesenteric resistance arteries (MrA) of male Wistar rats (±300gr) 2 weeks after sympathectomy with 6-hydroxydopamine (50 mg kg^{-1}, dissolved in 1 ml 0.9% NaCl (pH 4.7), 2 i.p injections at 3 hours interval on day 1 and day 7). At day 14, MrA were isolated, total RNA was extracted and SM α-actin mRNA levels were determined by competitive RT-PCR. All data were expressed as mean±SEM. Succesfull removal of the sympathetic nerve endings was demonstrated by a drastic reduction of glyoxylic acid induced histofluorescence in whole mount preparations of MrA. SM α-actin mRNA levels were reduced in sympathectomized rats (n=5) compared to sham-injected rats (n=4) (25±7vs.47±6 fg/ng total RNA, $p<0.05$, Student's t-test).

In a previous study we demonstrated a significant reduction in maximal active wall stress (mAWS) in MrA 5 weeks after myocardial infarction (MI) (Stassen et al., 1997). Since MI has been associated with sympathetic nerve depletion (Zelis et al., 1993), we hypothesized that this reduced mAWS post-MI may result from MrA VSMC dedifferentiation. MI was induced in male Wistar rats (±300gr) by permanent ligation of the left coronary artery while anaethetised with sodium pentobarbitone (60mg kg^{-1} i.p., n=7) (Stassen et al, 1997). Five weeks post-MI, catecholamines were extracted from isolated MrA and the noradrenaline content was measured by HLPC as an indicator of sympathetic nerve depletion. The expression of SM α-actin mRNA was determined as described in the sympathectomy experiment. Findings were compared to those in sham-operated animals (SHAM, n=5). No alterations in the arterial noradrenaline content (MI: 56.8±14.4 vs. SHAM 42.6±6.9 ng/μg DNA) or SM α-actin mRNA levels (MI 51±15 vs. SHAM 54±14 fg/ng total RNA) were observed. These results indicate (i) the applicability of competitive RT-PCR to quantify gene expression in small resistance-sized arteries, (ii) that sympathetic nerve depletion may result in VSMC dedifferentiation, and (iii) that the previously observed hyporeactivity in MrA post-MI is not due to dedifferentiation of MrA VSMC following depletion of perivascular sympathetic nerves.

Stassen, F.R.M., Fazzi, G.E., Leenders, P.J.A. et al. (1997). J. Cardiovasc. Pharmacol., 29, 780-788
Zelis, R., Clemson, B., Baily, R. et al. (1993). Cardiovasc. Res., 26, 933-938.

93P INHIBITION OF THE ACTIVITY OF POLY(ADP-RIBOSE) SYNTHETASE REDUCES CELL INJURY CAUSED BY HYDROGEN PEROXIDE IN RAT CARDIAC MYOBLASTS

Joanne Bowes, Julie Piper & Christoph Thiemermann The William Harvey Research Institute, St. Bartholomew's & The Royal London School of Medicine & Dentistry, Charterhouse Square, London.

Reactive oxygen species (ROS) contribute to the pathophysiology of ischaemia-reperfusion injury. In cultured cells ROS cause strand breaks in DNA, which trigger an energy-consuming repair process by activating the nuclear enzyme poly-(ADP ribose) synthetase (PARS). Excessive activation of PARS leads to cell death, and PARS inhibitors such as 3-aminobenzamide (3-AB) attenuate the cytotoxic effects of radicals in cultured cells (Schraufstatter *et al.*, 1986). Inhibition of the activity of PARS reduces the degree of necrosis caused by ischaemia and reperfusion of the rabbit heart (Thiemermann *et al.*, 1997). Here we investigate the effects of various compounds on PARS activity and cell injury of rat ventricular myoblasts (H9c2 cell line) in culture, exposed to hydrogen peroxide (H_2O_2).

H9c2 cells were cultured in 96 well plates containing DMEM (200 µl) supplemented with L-glutamine (3.5 mM) and 10% foetal calf serum (FCS) until they reached confluence. Cells were exposed to hydrogen peroxide (10 µM-10 mM) and cell injury was assessed by measuring the reduction of MTT (3-(4,5-dimethyliazol-2-yl)-2,5-diphenyltetrazolium bromide) to formazan (i.e. measure of mitochondrial respiration). To investigate the effects of PARS inhibitors on the cell injury caused by H_2O_2, cells were pre-incubated (10 min) in media (1% FCS) containing vehicle (saline/0.01% DMSO) or the following drugs: 3-aminobenzamide (3-AB, 3 mM); 3-aminobenzoic acid (3-ABA, 3 mM); 1,5-dihydroxyisoquinoline (ISO, 300 µM); nicotinamide (Nic, 3 mM); nicotinic acid (NicA, 3 mM). Cells were then exposed to H_2O_2 (1 mM) for 4 h (37 °C). PARS activity was measured at 0, 10, 30, 60 and 90 min after administration of H_2O_2 in H9c2 cells cultured (as above) in 6 well plates, using the method of Schraufstatter *et al.* 1986 (which measures the PARS-dependent incorporation of NAD into nuclear proteins). Experiments were performed in triplicate (n=4).(*p<0.05, ANOVA, Bonferroni post-hoc test).

Exposure of H9c2 cells to H_2O_2 caused inhibition of mitochondrial respiration in a time- and concentration-dependent manner. Exposure to H_2O_2 (1 mM) for 4 h reduced mitochondrial respiration to 7% of control (100%). Preincubation with 3-AB, ISO or Nic attenuated the fall in mitochondrial respiration caused by H_2O_2. In contrast, 3-ABA or NicA did not have any effect (See table). Exposure of H9c2 cells to H_2O_2 caused a maximal increase in PARS activity within 30 min. (basal activity: 15±2 pmoles NAD incorporated/10^6 cells/min, 1 mM H_2O_2:29±4) This increase in PARS activity was abolished by 3-AB (15±2*, 3 mM) or ISO (14±2*, 300 µM), but unaffected by 3-ABA (27±3, 3 mM).

Drug	Concentration	Mito. Resp. (% control)	n
control		100%	4
H_2O_2	1 mM	7±1%	4
3-AB	3 mM	45±6%*	4
3-ABA	3 mM	5±2%	4
ISO	300 µM	55±5%*	4
Nic	3 mM	46±9%*	4
NicA	3 mM	3±3%	4

This finding that agents which inhibit PARS activity also attenuate the reduction in mitochondrial respiration caused by H_2O_2 supports our view (Thiemermann *et al.*, 1997) that activation of PARS by ROS causes injury of cardiac myoblasts and, presumably, myocytes.

JB is the recipient of a BHF studentship (FS/96015). CT is the recipient of a BHF senior research fellowship(FS/96018).

Schraufstatter I. *et al.*, (1986). *Proc. Natl. Acad.Sci.*, 83, 4908-4912
Thiemermann, C. *et al.*, (1997). *Proc. Natl. Acad. Sci.*, 94, 678-683

94P INCREASED MYOCARDIAL TOLERANCE TO ISCHAEMIA 24 H AFTER ADENOSINE A_1 RECEPTOR STIMULATION: EVIDENCE FOR A ROLE OF THE ATP-SENSITIVE K^+ CHANNEL

G. F. Baxter, D. M.Yellon, The Hatter Institute for Cardiovascular Studies, Division of Cardiology, University College London Hospital & Medical School, London WC1E 6DB.

Brief sublethal periods of myocardial ischaemia enhance the tolerance of myocardium to a period of ischaemia 24-72 h later. This cytoprotective adaptation is known as delayed preconditioning or second window preconditioning (Yellon & Baxter, 1995). We have previously reported that the process of adaptation in rabbit myocardium is initiated by endogenous adenosine release (Baxter *et al.*, 1994). Bolus administration of the selective adenosine A_1 receptor agonist 2-chloro-N^6-cyclopentyladenosine (CCPA) mimics the effects of brief myocardial ischaemia and induces delayed myocardial protection 24-72 h later (Baxter & Yellon, 1997). The downstream effector mechanism of protection is unknown. Opening of the ATP-sensitive K^+ channel (K_{ATP}) during ischaemia is known to protect against ischaemic injury. We hypothesised a role for the channel in this form of cardioprotection. We examined the effect of pharmacological K_{ATP} channel blockade on the acquisition of delayed myocardial protection following CCPA in a rabbit model of acute myocardial infarction.

CCPA (100 µg/kg i.v.) or saline was administered to male New Zealand White rabbits (2.2-3.2 kg). After 24 h, the animals were anaesthetised with a combination of Hypnorm (Janssen) 0.15 ml/kg i.m. and pentobarbitone sodium (40 mg/kg i.v.). The sternum was opened and a silk suture positioned around a proximal branch of the left coronary artery. The artery was occluded for 30 minutes followed by 120 minutes reperfusion The effect of K_{ATP} channel blockade was assessed using glibenclamide (gli; 0.3 mg/kg) and sodium 5-hydroxydecanoate (5HD; 5 mg/kg). These inhibitors or vehicle (Veh) were given i.v. 15 minutes before coronary occlusion. Myocardial risk zone (R) was delineated with fluorescent microspheres and the zone of infarction (I) was determined using triphenyltetrazolium staining. Computerised planimetry was employed to quantify these variables (Baxter *et al.*, 1994).

Table 1. Infarct size data

Treatment	n	I (cm^3)	R (cm^3)	I/R (%)
Saline + Veh	10	0.40±0.08	1.0±0.1	39.6±2.6
CCPA + Veh	11	0.23±0.05	1.0±0.1	23.4± 3.3*
Saline + Gli	6	0.47±0.09	1.1±0.1	42.7±5.5
CCPA + Gli	7	0.41±0.08	1.1±0.1	37.4±4.7†
Saline+ 5HD	5	0.41±0.08	1.0±0.1	42.0±5.8
CCPA+ 5HD	6	0.39±0.05	0.8±0.1	48.8±3.7†

Mean ± s.e. mean. * $P < 0.05$ vs S + Veh group; † $P < 0.05$ vs C + Veh group (1-way ANOVA)

CCPA pretreatment increased resistance to myocardial infarction 24 h later. This protection concorded with our previous observations and was independent of risk zone volume, heart rate and blood pressure. Blockade of K_{ATP} with either gli or 5-HD prior to coronary occlusion abolished the protection induced by CCPA. This suggests that K_{ATP} opening plays an essential role in A_1 receptor-induced delayed protection. We conclude that adaptive cytoprotection induced by transient A_1 receptor activation is dependent on K_{ATP} channel opening during ischaemia-reperfusion. However, the precise mechanism by which A_1 receptor activation modifies ion channel activity sub-acutely remains to be determined.

G. F. Baxter is supported by the British Heart Foundation.

Baxter G.F., Marber M.S., Patel V.C. & Yellon D.M. (1994). *Circulation*, 90, 1993-2000.
Baxter G.F. & Yellon D.M. (1997). *J. Cardiovasc. Pharmacol.* 29, 631-638.
Yellon D.M. & Baxter G.F. (1995). *J. Mol. Cell. Cardiol.* 27, 1023-1034

95P ACE- AND CHYMASE-DEPENDENT ANGIOTENSIN I-TO-II CONVERSION IN THE HUMAN ISOLATED CORONARY ARTERY

A. MaassenVanDenBrink, P.R. Saxena & A.H.J. Danser, Department of Pharmacology, Erasmus University Rotterdam, The Netherlands.

Studies in homogenates prepared from human cardiac tissue have suggested that conversion of angiotensin I (AngI) into AngII is mediated by human heart chymase rather than angiotensin-converting enzyme (ACE) (Urata *et al.*, 1990). Heart chymase-dependent AngII formation is strongly inhibited by the natural protease inhibitor α_1-antitrypsin, present in both blood and interstitial fluid (Kokkonen *et al.*, 1997). In the present study we quantified ACE- and chymase-dependent AngI-to-II conversion in the human isolated coronary artery. In addition, we investigated the inhibitory effect of α_1-antitrypsin in this preparation. Ring segments of right epicardial coronary artery (9 heart valve donors; 5 M, 4 F; 5-53 yr) were suspended in organ baths. Tension was recorded isometrically and was expressed as percentage of the contraction to 100 mM K^+. Experiments were performed in a paired parallel setup. Functional integrity of the endothelium, expressed as relaxation to substance P (1 nM), was 59±10% of precontraction to prostaglandin $F_{2\alpha}$ (1 μM). Concentration response curves to AngI or AngII (0.1 nM - 1 μM) were constructed in the presence or absence of either the ACE inhibitor captopril (100 μM), the chymase inhibitor chymostatin (100 μM) or α_1-antitrypsin (0.5 and 1.0 mg/ml). Ang I and Ang II displayed a similar maximal effect ($E_{max,Ang}$ 26±9% and 22±4%, respectively), but AngI was less potent than AngII (pD_2: 7.4±0.2 and 8.0±0.1, respectively, n=5). From these data it can be estimated that 33±13% of AngI is converted to AngII ((EC_{50} AngII/ EC_{50} AngI)*100%). Since in the presence of the inhibitors, concentration response curves did not always reach $E_{max,Ang}$ (contraction at 1 μM AngI: 21±6% for control, 16±5% with captopril, 7±1% with chymostatin, 18±5% with 0.5 mg/ml α_1-antitrypsin, n=7), the potency of AngI under these conditions could not be determined. We therefore calculated the concentration of AngI required to obtain 5% of the K^+-induced contraction ($E_{5\%K+}$), corresponding to about 25% of $E_{max,Ang}$ (Table 1). Both with captopril and chymostatin the concentration of AngI required to induce $E_{5\%K+}$ was approximately tenfold higher than without these inhibitors. α_1-antitrypsin did not affect the AngI response. We conclude that ACE and chymase play an equally important role in the conversion of AngI-to-II in our preparation. α_1-antitrypsin does not appear to inhibit chymase-dependent AngI-to-II conversion in the intact human isolated coronary artery.

Kokkonen, J.O., Saarinen, J. & Kovanen, P.T. (1997). *Circulation* 95, 1455-1463.
Urata, H., Healy, B., Stewart, R.W. *et al.* (1990). *Circ. Res.* 66, 883-890.

Table 1. AngI concentration required to induce $E_{5\%K+}$ (mean±s.e.mean)

	n	-Log[AngI] (M)
AngI (control)	9	7.9±0.1
AngI + captopril	7	7.0±0.2†
AngI + chymostatin	7	6.9±0.3†
AngI + α_1-antitrypsin (0.5 mg/ml)	7	7.4±0.2
AngI + α_1-antitrypsin (1.0 mg/ml)	3	7.7±0.4

†) Significantly different from control ($P<0.05$; paired t-test)

96P THE PRESSOR RESPONSE EVOKED BY ACTIVATION OF FOREBRAIN 5-HT_{2A} RECEPTORS INVOLVES THE ACTIVATION OF CENTRAL AT_1 RECEPTORS IN ANAESTHETISED RATS

I.D. Knowles & A.G. Ramage, Academic Department of Pharmacology, Royal Free Hospital School of Medicine, Rowland Hill St., Hampstead, London. NW3 2PF.

5-HT, administred i.c.v. in rats, causes a rise in blood pressure and the release of vasopressin by activating central 5-HT_2 receptors (Anderson *et al.*,1991, Pergola *et al.*, 1992). Angiotensin II, i.c.v., also causes the release of vasopressin (Keil *et al.*, 1975). Experiments were, therefore, carried out to investigate whether the pressor response evoked by the 5-HT_2 receptor agonist quipazine (Knowles *et al.*,1997) is mediated by central AT_1 receptors.

In male Sprague-Dawley rats (250-375 g) anaesthesia was induced with isoflurane and maintained with α-chloralose (80 mg kg^{-1} plus supplementary doses of 10 mg kg^{-1} as required). Rats were artificially ventilated following neuromuscular blockade with decamethonium (3 mg kg^{-1}). Simultaneous recordings were made of blood pressure, heart rate and renal and phrenic nerve activities. Blood gases, pH and rectal temperature were also monitored and maintained within the normal physiological range (see Anderson *et al.*, 1992). All experiments were carried out in the presence of 0.1 mg kg^{-1} i.v. of BW501C67 (Anderson *et al.*, 1992). Drugs were given i.c.v. in a volume of 5 µl over 15s. Changes were compared with vehicle control (which had been pretreated i.c.v. with antagonist vehicle; 10% polyethylene glycol 400 (PEG)) by two-way ANOVA and the least significant difference test was used to compare the means. All values are means ± s.e.mean.

Quipazine i.c.v. (2 µmol kg^{-1}, n=8) caused a significant (P <0.05) rise, after 3 min, of 15±4 mmHg in BP and 29±9 beats min^{-1} in HR and renal sympathoinhibition of -21±11%. Injection, i.v., of the vasopressin V_1 antagonist ($d(CH_2)_5Tyr(Me)AVP$, 30 µg kg^{-1}, n=6) at 3 min, caused BP to fall, reaching baseline values after 2 min, and reversed the sympathoinhibition to excitation of +22± 24% after 3 min. Losartan i.c.v. (1 and 4 µg kg^{-1}, n=5) inhibited the quipazine induced rise in BP but not the rise in HR, and reversed the sympathoinhibition to excitation. The sympathoexcitation was greater for the 4 µg kg^{-1} dose, 66±22% c.f. 43±12%. Spiperone i.c.v. (10 and 30 nmol kg^{-1}; n=5) attenuated all the effects of quipazine. Interestingly, quipazine, in the presence of 30 nmol kg^{-1} spiperone, caused an initial, small and significant, fall in BP of -7±5 mmHg compared to PEG alone.

It is concluded that the rise in BP, due to activation of central 5-HT_{2A} receptors, is mediated by central AT_1 receptors. However, AT_1 receptors are not involved in the tachycardia evoked by activation of central 5-HT_{2A} receptors, or the central renal sympathoexcitatory response which is uncovered when vasopressin release is inhibited. Finally, the data support the view that central 5-HT_{2A} receptor mediated release of vasopressin involves a central angiotensinergic pathway (Saydorff *et al.*, 1996).

I.D.K is a MRC student.

Anderson, I.K. *et al.* (1992) *Br. J. Pharmacol.* **107**, 1020-1028.
Keil, L.C. *et al.* (1975) *Endocrinology*, **96**, 1063-1065.
Knowles, I.D. *et al.* (1997) *J. Physiol.* **501**, 71P.
Pérgola, P.E. *et al.* (1993) *Neuroendocrinology*, **57**, 550-558.
Saydorff, J.A. *et al.* (1996) *Am. J. Physiol.* **270**, E513-E521.

97P EARLY CAPTOPRIL TREATMENT OF RATS PREVENTS INFARCTION-INDUCED HYPERTROPHY BUT NOT ANGIOGENESIS: EFFECTS ON TISSUE PERFUSION AND METABOLISM

R.G. Schoemaker, P. van Haren, P.R. Saxena, E.A.J. Kalkman, Department of Pharmacology, Faculty of Medicine and Health Sciences, Erasmus University Rotterdam, P.O. Box 1738, 3000 DR Rotterdam, The Netherlands.

Delayed captopril treatment, started after the healing phase of myocardial infarction (MI), improves perfusion by reducing tissue weight without affecting vascular capacity of the heart, thus preserving aerobic metabolism (Kalkman *et al.*, 1996). This delayed treatment is generally associated with improved prognosis. Early captopril treatment, of which prognostic effects are still questionable, prevents reactive hypertrophy (Schoemaker *et al.*, 1991). However, if this effect is accompanied by prevention of vascular growth, tissue perfusion will not improve. The present study examines this question by evaluating the effects of early captopril treatment on regional coronary flow related to tissue mass. Wistar rats, subjected to coronary artery ligation, received drinking water with or without captopril (2 g/l, from 1 day until 3 weeks after MI). Reactive hypertrophy was confined to the spared part of the left ventricular free wall (12% increase in weight, despite replacement of the major part by scar tissue), which was prevented by captopril. Neither global maximal vascular capacity during nitroprusside induced vasodilation (sham: 20.7 ± 0.7; MI: 19.9 ± 0.9; MI+captopril: 20.1 ± 0.8 ml/min, n=9-13), nor its regional distribution, measured in isolated perfused hearts, using radioactive microspheres, were affected by captopril. Prevention of hypertrophy without suppression of maximal capacity resulted in normalization of the MI-induced reduction in global cardiac perfusion (sham: 20.2 ± 0.8; MI: 17.1 ± 0.8; MI + captopril: 21.9 ± 1.0 ml/min.g), and regionally in the left ventricular free wall (27 % increase) and the septum (33 %increase). In MI hearts studied in parallel, the metabolic consequences were evaluated by measuring the release of purines (ATP-catabolites) and lactate into the coronary effluent. In MI heart purines release was significantly reduced (sham: 17.3 ± 3.7; MI: 11.7 ± 1.7 nmol/min.g, n=5-7) at normal lactate levels (sham: 483 ± 68; MI: 561 ± 91 nmol/min.g). Captopril restored the increased lactate/purine ratio (sham: 29.8 ± 2.9; MI: 48.6 ± 4.8) to sham values (MI +. captopril: 26.9 ± 2.6), by reducing lactate release (259 ± 32 nmol/min.g) without affecting purines release (9.7 ± 1.0 nmol/min.g), indicating a better preservation of aerobic metabolism. Light microscopic examination of resistance arteries revealed no effect on wall to lumen ratios (MI: 0.68 ± 0.08; MI + captopril: 0.62 ± 0.09, n=6-7) nor on average lumen diameter (MI: 78 ± 5; MI + captopril: 72 ± 5 μm) in vessels in viable tissue, whereas the pronounced increase in wall to lumen ratio in vessels in the infarct scar (3.36 ± 0.41, at an average lumen of 59 ± 3 μm) was partly normalized by captopril (wall/lumen: 1.90 ± 0.34, at a lumen of 77 ± 6 μm). This suggests that captopril does not affect vessel structure in the viable myocardium. These data indicate that early captopril prevented post-MI hypertrophy but not angiogenesis, thus beneficially influencing the vascularisation/tissue mass ratio, probably reflected in preservation of aerobic metabolism.

Kalkman, E.A.J. *et al.* (1996). *Eur. J. Pharmacol.* **298,** 121-128

Schoemaker, R.G. *et al.* (1991). *J. Mol. Cell. Cardiol.* **23,** 187-197

98P EFFECT OF ELEVATED GLUCOSE LEVELS ON THE VASCULAR REACTIVITY OF THE *EX VIVO* MESENTERIC ARTERIAL BED OF SPONTANEOUSLY HYPERTENSIVE AND WISTAR-KYOTO RAT STRAINS

R Monkhouse, N Ashton*, I Gouldsborough*, S Rossiter, BC Williams Dept. Medicine, Western General, Edinburgh, EH4 2XU. * School of Health Sciences, University of Sunderland, SR1 3SD.

The association between diabetes and hypertension is well established. Insulin resistance occurs in humans with hypertension and in the spontaneously hypertensive rat (SHR; Tsutsu et al., 1989) leading to impaired regulation of blood glucose. In the present study, the mesenteric arterial bed of the SHR was exposed to perfusate containing elevated glucose, to mimic hyperglycaemia. Age-matched Wistar-Kyoto (WKY) rats were used as normotensive controls.

Systolic blood pressure (SBP) was measured in SHR and WKY rats by tail-cuff plethysmography at 14-24 weeks of age. The mesenteric arterial beds were isolated under anaesthetic and perfused (3ml/min - 37° C) with Krebs-Ringer buffer (95%O_2 /5%CO_2) containing either normal glucose (ng-11.11mM) or high glucose (hg-32.8mM). Perfusion pressure (mmHg) was measured continuously in response to the vasoconstrictors noradrenaline (NA;0.1μM-20μM) and vasopressin (AVP;0.1nM-20nM) and following pre-constriction with 0.3μM NA, to the vasodilators acetylcholine (ACh;0.1nM-0.1mM) and glyceryl trinitrate (GTN;0.1nM-1μM). Maximal (Max) vasoconstriction and vasodilatation responses and pEC_{50} values were calculated and presented as the mean±sem (Table 1). Statistical analysis was performed by oneway ANOVA and Student Newman Keuls test or Student's independent t-test, as appropriate.

WKY had significantly lower SBP than SHR (157±2mmHg vs 230±3mmHg). SHR mesenteries exhibited higher Max. responses to NA ($P<0.0001$) and AVP ($P<0.005$) when compared with WKY. Glucose concentration had no significant effect on the maximal responses to NA or ACh in either strain. Both SHR and WKY mesenteries perfused with hg buffer, showed an enhanced maximal vasodilatory response to GTN when compared with ng perfusions ($P=0.049$ and $P=0.0075$) respectively. AVP-induced Max. vasoconstriction was enhanced in WKY mesenteries perfused with hg vs ng ($P=0.0059$). This was not seen in the SHR which exhibited an impaired pressor response to AVP when perfused with hg ($p=0.0127$). The pEC_{50} values were comparable between perfusion preparations.

In conclusion, vascular reactivity of the mesenteric artery is altered in hypertension and by glucose, which is not due to changes in osmolality. The enhanced vasoconstrictor effect of NA in the SHR is due to hypertension but not glucose, whilst the response to AVP in the SHR is influenced by both hypertension and glucose. GTN-induced vasodilatation is enhanced by glucose not hypertension. Neither hypertension nor hg affects the vascular response to ACh, however there is a trend towards greater vasodilatation with high glucose.

Tsutsu N, Takata Y *et al* (1989). *Metabolism*, 38. 63-66

Table 1:Mean ± sem for maximum responses and pEC_{50} values. Depressor actions of Ach and GTN were expressed as the percentage decrease of the pre-constriction pressure of 3μM NA. + Denotes significant differences between strains and * for significance between glucose concentrations.

GROUP	NA-MAX	NA- pEC_{50}	AVP-MAX	AVP- pEC_{50}	ACh-MAX	ACh- pEC_{50}	GTN-MAX	GTN-
SHR (ng)	260.6±16.9 +	6.1±0.06	251.3±22.9 + *	8.8±0.06 +	32.4±3.15	7.4±0.24	51.9±7.23 *	7.8±0.31
SHR (hg)	245.6±16.2	5.9±0.05	184.9±14.4	8.6±0.08	52.1±8.93	7.4±0.34	70.4±4.44	7.7±0.28
WKY (ng)	154.9±12.6	6.0±0.15	124.4±8.08 *	9.2±0.06	33.1±6.6	6.5±0.25	36.3±5.63 *	7.3±0.25
WKY (hg)	153.1±11.8	5.8±0.09	149.9±4.95	9.0±0.09	44.2±7.71	7.0±0.41	63.2±6.74	7.3±0.19

99P ENDOTHELIAL CELL DYSFUNCTION IN RESISTANCE ARTERIES FROM DIABETIC AND NON-DIABETIC BIOBRED RATS

P.W.F.Hadoke[1], B.C.Williams[2], J.D.Baird[1] & R.M.Lindsay[3]. [1]Dept. Medicine, Royal Infirmary, Edinburgh, EH3 9YW, [2]Dept. Medicine and [3]Metabolic Unit, Western General, Edinburgh, EH4 2XU.

Impaired vascular smooth muscle (VSM) and endothelial cell (EC) function has been in demonstrated in resistance arteries from patients (McNally *et al.*, 1994) and animals (Heygate *et al.*, 1995) with diabetes. Few studies have investigated vascular abnormalities in resistance arteries from the spontaneously diabetic BioBred (BB) rat. This investigation aimed to determine whether resistance artery function was impaired in BB rats with established diabetes.

Vascular function was assessed in mesenteric arteries from male diabetic (age 179±8 days, wt.426±7g; daily insulin dose 2.5±0.1U; n=8) and matched, non-diabetic BB rats (age 182±5 days, wt.405±16g; n=8). Third order mesenteric arteries from these rats were mounted in a myograph chamber containing physiological salt solution, maintained at 37°C and perfused with 95%O_2; 5%CO_2 (pH 7.4), for measurement of isometric responses. Following equilibration at their optimum resting force ($0.9L_{100}$) and a standard start procedure (Aalkjaer *et al.*, 1987) cumulative concentration-response curves were constructed for the vasoconstrictors noradrenaline (NA, 10^{-9}-$3x10^{-5}$M), arginine vasopressin (AVP; 10^{-12}-$3x10^{-7}$M) and endothelin-1 (ET-1; 10^{-11}-$3x10^{-6}$M). Vasodilator responses were investigated, following sub-maximal contraction with NA ($3x10^{-6}$M), using the endothelium-dependent vasodilators acetylcholine (ACh; 10^{-9}-$3x10^{-5}$M) and bradykinin (BK; 10^{-10}-$3x10^{-6}$M), and the endothelium-independent nitric oxide donor 3-morpholinosydnonimine (SIN-1; 10^{-9}-$3x10^{-5}$M). Results are mean ± s.e.mean. Comparisons were performed using Student's t-test.

Diabetic BB rats had significantly higher plasma glucose (22.3±3.8 vs 6.6±0.1mmol/l; P<0.01) and glycated haemoglobin (9.6±1.1 vs 3.8±0.1%; P<0.001), but not cholesterol (2.5±0.09 vs 2.36±0.11 mmol/l; P>0.1) concentrations than non-diabetic BB rats. The internal diameter (i.d.) of arteries from diabetic BB rats (i.d. 265±17μm) was smaller, although not significantly (P=0.30), than that of arteries from non-diabetic (i.d. 290±17μm) BB rats. Arteries from both groups relaxed in response to the endothelium-independent agonist, SIN-1 (Table 1). Endothelium-dependent responses to ACh and BK, however, were small in both diabetic and non-diabetic BB rats, with sensitivity to ACh significantly lower in diabetic animals (Table 1). Arteries did not relax sufficiently in response to BK to allow calculation of sensitivity (pD_2) values. Maximum contraction and sensitivity to vasoconstrictors tended (not significant) to be smaller in vessels from diabetic, compared with non-diabetic, BB rats (Table 1).

Endothelium-dependent, but not endothelium-independent, relaxation in both diabetic and non-diabetic BB rats was smaller than would be expected from third order branches of rat mesenteric arteries (McIntyre *et al.*, 1996). This suggests EC dysfunction in non-diabetic, as well as diabetic, BB rats. Similar results have been obtained with carotid arteries from these animals (Hadoke *et al.*, 1997). These results indicate that development of diabetes is not the sole factor responsible for the EC dysfunction demonstrated in this model.

Aalkjaer,C., Heagerty,A., Petersen,K.*et al.*(1987) *Circ.Res.*,61, 181-6.
Hadoke P.W.F, Williams, B.C., Baird, J.D. *et al.*, 1997, this meeting.
Heygate,K.M., Lawrence,I.G. *et al.*(1995) *Br.J.Pharmacol.*, 116, 3251-9.
McIntyre, C-A., Williams, B.C. *et al.*, 1996, *Br.J.Pharmacol.*, 119, 318P.
McNally, P.G., Watt, P.A.C., Rimmer, T. *et al.*, (1994) *Clin.Sci.*, 87, 31-36.

Table 1. Maximum relaxation (M.R.; %), maximum contraction (M.C.; mN/mm) and sensitivity (pD_2) data for diabetic and non-diabetic BB rats.

	ACh		SIN-1		BK		NA		AVP		ET-1	
	M.R.	pD_2	M.R.	pD_2	M.R.	pD_2	M.C.	pD_2	M.C.	pD_2	M.C.	pD_2
Non-diabetic	56.3+11.0	7.46+0.17	89.5+4.6	5.36+0.27	34.5+6.8	----[a]	3.33+0.53	6.06+0.06	3.22+0.50	9.61+0.18	2.85+0.43	8.78+0.21
Diabetic	36.1+6.7	6.97+0.12	95.2+1.5	5.42+0.24	30.7+6.2	----[a]	2.91+0.44	5.91+0.15	2.65+0.47	9.47+0.06	2.46+0.37	8.57+0.14
P	0.14	0.03*	0.25	0.88	0.68		0.54	0.39	0.42	0.50	0.51	0.41

Results are mean ± s.e.mean.* denotes significant difference (P<0.05, Student's t-test). [a] could not be calculated.

100P DIVERSE EFFECTS OF ANGIOTENSIN PEPTIDES IN RABBIT ISOLATED RENAL ARTERY

Q. Li, M. Pfaffendorf & P.A. van Zwieten, Dept. of Pharmacotherapy, AMC, University of Amsterdam, Meibergdreef 15, 1105 AZ Amsterdam, The Netherlands

Angiotensin III (AIII) and angiotensin (1-7) are the N-terminal and C-terminal degradation products of angiotensin II (AII), respectively. Elevated levels of these two peptides have been expected and indeed observed in the anti-hypertensive treatment with selective AT_1-receptor antagonists. Previous study by our group has shown a non-competitive antagonism of losartan on AII-induced responses in this preparation (Zhang *et al*, 1994). In the present study, the effects of AIII and angiotensin (1-7), were investigated and compared with those of AII in isolated rabbit renal artery (RA) preparations.

Male New Zealand white rabbits weighing 1.5 - 2.0 kg were used in this study. The rabbits were killed by exsanguination after intravenous injections of fentanyl citrate (0.25 mg kg^{-1}), fluanisone (7.5 mg kg^{-1}) and heparin (100 IU kg^{-1}). Left RA were isolated and cut into rings of 3 mm length. Endothelium was destroyed by gently rubbing the intimal surface of the vessels with a small wooden rod. Vascular rings were set up in a 10 ml organ bath with Krebs' solution at 37°C and gassed with 95% O_2 + 5 % CO_2. Changes in isometric force were recorded and a resting tension of 2 g was maintained. Two cumulative concentration-response curves (CRC) for AII or AIII were established after an interval of 1 h. In some experiments, the selective AT_1-receptor antagonist irbesartan was added 30 min before the second series of CRCs were constructed. In other experiments, angiotensin (1-7) alone or combined with the cyclooxygenase inhibitor indomethacin, the selective AT_1-receptor antagonist losartan or the selective AT_2-receptor antagonist PD123177 (1-[(4-amino-3-methylphenyl) methyl]-5-(diphenyl-acetyl)-4,5,6,7-tetrahydro-1H-imidazole[4,5-C] pyridine-6-carboxylic acid), respectively, were added 30 min before the construction of the second series of curves. Tachyphylaxis for AII or AIII were not observed in the present study.

Data are expressed as absolute values (g) or percentages of the first maximal responses. All drugs were dissolved in saline except for indomethacin and PD123177, which were taken up in a small volume of 0.1 M Na_2CO_3 and 1 M NaOH, respectively, and subsequently diluted with saline. Data are presented as means ± s.e.mean for *n* observations. The statistical significance of differences was evaluated by means of one-way analysis of variance (ANOVA) or two-sided Student's *t* test. Statistical significance was assumed for values of $P < 0.05$.

In RA preparations, (0.3 - 30 nM) AII and (0.3 - 100 nM) AIII caused concentration-dependent contractions with comparable maximal responses (E_{max}: 3.26 ± 0.14 g and 3.34 ± 0.07 g, respectively; $P > 0.05$; $n = 5 - 8$). AIII was about 2 times less active than AII (pD_2: 8.16 ± 0.03 and 8.56 ± 0.05, respectively; $P < 0.05$; $n = 5 - 8$). Irbesartan (3 - 30 nM) concentration-dependently shifted the CRCs for AII and AIII to the right and reduced the maximal contractions (pK_B: 9.14 ± 0.09 and 9.36 ± 0.13, respectively; $P > 0.05$; $n = 4 - 5$). The residual AII- and AIII-induced contractions in the presense of 30 nM irbesartan amounted to 47.7 ± 1.5% and 66.7 ± 1.9%, respectively, of the maximal responses obtained in the absence of irbesartan ($P < 0.05$; $n = 5$). Angiotensin (1-7) caused neither contraction nor relaxation in this preparation. However, (1 - 30 μM) angiotensin (1-7) concentration-dependently shifted the CRCs for AII and AIII to the right and reduced the maximal contractions (pK_B: 6.14 ± o.11 and 5.93 ± 0.13, respectively; $P > 0.05$; $n = 5 - 7$). Co-incubation with 1 μM indomethacin or PD123177 did not significantly influence the effects of 10 μM angiotensin (1-7) on AIII-induced contractions (E_{max}: 20.3 ± 2.1%, 20.9 ± 2.1% and 21.4 ± 2.4%, respectively; $P > 0.05$; $n = 4 - 5$). Losartan (10, 30 and 100 nM) concentration-dependently reversed the decreased maximal responses to AIII (E_{max}: 68.8 ± 2.7%, 81.3 ± 2.0% and 105.2 ± 2.2%, respectively; $P < 0.05$; $n = 4 - 6$).

Our results indicate that in rabbit RA preparations, AII and AIII are similarly efficacious vasoconstrictor agents. Their effects are mediated by AT_1-receptors, and there might exist multiple AT_1-receptor subtypes in this preparation. Angiotensin (1-7) acts as an antagonist of AII- and AIII-induced contractions. This inhibitory effect is mediated via AT_1-receptors. Prostaglandins seem not to be involved.

Zhang, J., Pfaffendorf, M., Zhang J.S. & van Zwieten, P.A. (1994) *Eur. J. Pharmacol.* 252, 337-340.

101P K^+ CHANNELS DETERMINING THE MEMBRANE POTENTIAL OF RABBIT RENAL ARCUATE ARTERY

H. M. Prior, M. S. Yates and D. J. Beech
Department of Pharmacology, University of Leeds, Leeds, LS2 9JT.

The membrane potential is a critical determinant of excitability in many cell types including arterial smooth muscle cells. In this study we have investigated the functions of different K^+ channel types in governing the membrane potential of renal arcuate arteries.

Intact arteries from male, Dutch rabbits (1-1.5 kg) were pressurised to 60 mmHg and lumenal diameter measured using video microscopy. Membrane potential was measured from smooth muscle cells freshly isolated from arteries, using amphotericin-perforated patch recording. Values are given as mean ± s.e.mean.

Superfusion with iberiotoxin at 0.1 then 1 μM constricted arteries by 23.2 ± 5.5 % (n=6) and 32 ± 6.4 % (n=4) respectively. Similarly, 1 mM TEA^+ constricted arteries by 21.1 ± 8.3 % (n=11), as did 0.01, 0.1 and 1 mM Ba^{2+}, which constricted arteries by 6.6 ± 4.5 % (n=8), 23 ± 7.1 % (n=8) and 28.4 ± 13.6 % (n=6). In contrast, application of 0.1 μM apamin (n=6), 1 μM glibenclamide (n=11) or 1 mM 3,4 diaminopyridine (n=6) had no effect.

The membrane potential of isolated smooth muscle cells was -38 ± 2 mV (n=60). Elevation of the extracellular K^+ concentration from 5 to 130 mM depolarised cells by 37.6 ± 4.7 mV (n=9) whereas application of 1 mM 4,4'-diisothiocyanato-stilbene-2,2'-disulfonic acid had no significant effect (2.5 ± 2.5 mV, n=4). Iberiotoxin (0.1 μM) had no effect on membrane potential (n=8) but did inhibit spontaneous transient hyperpolarisations (3 out of 3 cells). 3,4 Diaminopyridine had no effect on membrane potential (n=3) but did inhibit rectification observed on injection of depolarising current (n=3) and attenuated K_V channel current at 0 mV by 55.7 ± 7 % (n=11) in voltage-clamp recordings. Also, a cocktail containing 1 mM 3,4 diaminopyridine, 0.1 μM apamin, 1 μM glibenclamide and 10 μM ouabain had no effect on membrane potential (n=5). In 10 cells to which 1 mM Ba^{2+} was applied, 6 depolarised by 15.3 ± 5.2 mV and the others were unresponsive. In voltage-clamp recordings an iberiotoxin-resistant K^+-current was present in some cells and this was inhibited by 0.1-10 mM Ba^{2+}. In 4 cells bathed in 60 mM K^+ solution, the Ba^{2+}-sensitive current was voltage-independent between 0 and -60 mV and had a mean amplitude of -53 ± 5.7 pA at -60 mV.

The data suggest the membrane potential is not influenced by K_{ir}, K_{ATP}, aminopyridine-sensitive K_V or apamin-sensitive K^+ channels. Maxi K^+ (BK_{Ca}) channels play a role, but only during spontaneous transient hyperpolarisations. An apparently novel voltage-independent K^+ channel appears to have direct influence on the membrane potential.

The work was supported by the Wellcome Trust.

102P CLONING OF A K_{ATP} CHANNEL FROM HUMAN AORTA

S. Narwal, D. McHugh, R.L. McDonald, D.J. Beech and A. Sivaprasadarao Department of Pharmacology, University of Leeds, Leeds, LS2 9JT

Electrophysiological recordings from vascular smooth muscle cells suggest the existence of several types of K_{ATP} channel with differing unitary conductance, regulation by nucleotides, and pharmacology. K_{ATP} channels cloned from insulinoma cell-lines are comprised of an α pore-forming subunit (Kir6) and a regulatory β subunit (sulphonylurea receptor, SUR1). Both subunits are required for channel function.

In an attempt to isolate a vascular smooth muscle K_{ATP} channel cDNA, we have screened a human aorta cDNA library under low stringency using as a probe rat pancreatic uK_{ATP-1} (Inagaki *et al.*, 1995a). Two cDNA clones were isolated of 2.4 kb and 1.8 kb. The 2.4 kb cDNA was sequenced and has an open reading frame encoding a 424 amino acid protein and shares 100%, 97% and 71% amino acid sequence identities with human lung K_{ATP} (Inagaki *et al.*, 1995b), uK_{ATP-1}, and Kir6.2 (Inagaki *et al*, 1995c) channels. Thus it belongs to the Kir6 family and is designated hK_{ATP}. hK_{ATP} contains the GFG pore-motif that is found in other Kir6 proteins and two putative transmembrane-spanning domains. hK_{ATP}, Kir6.2 and SUR1 cDNAs were subcloned into the pKSglobin vector and cRNA was prepared for micro-injection into defolliculated *Xenopus Laevis* oocytes. Two-electrode voltage-clamp recordings were made 24-48 hours after injection. The bath solution during recordings contained (mM): 90 KCl, 1.8 CaCl2, 1 MgCl2, 5 Hepes (pH 7.4). A 1-s ramp change in voltage from -120 to +70 mV was applied every 10 s.

Bath application of 3 mM sodium azide induced a mean (+ s.e.mean) current, at -100 mV, of -0.41 ± 0.17 μA in hK_{ATP}, and SUR1 co-injected oocytes (n=6), compared with -0.78 ± 0.22 μA for Kir6.2 and SUR1 (n=6). In hK_{ATP} and SUR1 co-injected oocytes the response to azide reached a maximum after 8 ± 1.3 min (n=6), compared with 10 + 2.1 min for Kir6.2 and SUR1 (n=5). Diazoxide (0.2 mM), applied in the presence of azide, induced additional current, increasing the azide-induced current by 126.4 ± 31.4% for hK_{ATP} and SUR1 (n=5) and 103 ± 38.3% for Kir6.2 and SUR1 (n=5). Glibenclamide (1 μM) inhibited the azide and diazoxide-induced current by 113.4 ± 4.2% for hK_{ATP} and SUR1 (n=6) and 102 ± 5% for Kir6.2 and SUR1 (n=6). No currents were observed for oocytes injected with only SUR1 (n=4) or only hK_{ATP} (n=8). Thus, a Kir6.1 homologue has been cloned from human aorta. When expressed in *Xenopus* oocytes with SUR1 it forms a functional channel which is activated by metabolic inhibition and diazoxide and inhibited by glibenclamide.

The work is supported by a BBSRC PhD Studentship (S Narwal) and by the MRC.

Inagaki, N., Tsuura, Y., Namba, N. *et al.* (1995a). *J. Biol. Chem.* 270, 5691-5694.
Inagaki, N., Gonoi, T., Clement, J.P. *et al.* (1995b). *Science* 270, 1166-1170.
Inagaki, N., Inazawa, J. & Seino, S. (1995c) *Genomics 30*, 102-104.

103P INHIBITION OF HUMAN P2X, RECEPTOR-MEDIATED YO-PRO-1 INFLUX BY PPADS AND KN62

A.D. Michel, I.P. Chessell & P.P.A. Humphrey. Glaxo Institute of Applied Pharmacology, Dept. of Pharmacology, University of Cambridge, Cambridge CB2 1QJ.

The human $P2X_7$ receptor is the most recently identified member of the P2X family of ion-channel receptors (Rassendren et al., 1997). The initial studies on the human $P2X_7$ receptor (Rassendren et al., 1997) suggest that it is only weakly inhibited by the available P2X receptor antagonists. However a more recent study suggests that KN62 is a potent $P2X_7$ receptor antagonist (Garget et al., 1997). In the present study we have confirmed the ability of KN62 to antagonise $P2X_7$ receptor mediated effects and have identified PPADS (pyridoxalphosphate-6-azo-phenyl-2',4'-disulphonic acid) as a potent antagonist of the human $P2X_7$ receptor.

Studies were performed using HEK293 cells stably transfected with the human recombinant $P2X_7$ receptor. Receptor function was assessed by measuring dibenzoyl-ATP (DbATP) stimulated YO-PRO-1 influx fluorometrically over a 30 min period as described elsewhere (Michel et al., this meeting). A buffer of the following composition (mM) was utilised :- 10 Hepes, 10 glucose, 5 KCl, 0.5 $CaCl_2$, 280 sucrose (pH 7.4 at 37°C). Data are the mean ± s.e.mean of 3-5 experiments. Values that differ significantly ($p<0.05$; Duncan's test) from control values are indicated by an asterix.

Following a 30min preincubation, PPADS and KN62 insurmountably inhibited DbATP-stimulated YO-PRO-1 influx. Thus, in control cells the DbATP pEC_{50} was 6.4±0.1. In the presence of 10 and 100 nM PPADS pEC_{50} values were 6.1±0.1* and 5.6±0.1*, respectively. In the presence of 10 and 100 nM KN62 pEC_{50} values were 6.1±0.1* and 5.8±0.1*, respectively. Schild analysis could not be used since the maximum response was reduced (i.e. maximal responses in the presence of 10 and 100 nM PPADS and 10 and 100 nM KN62 were 79±4*, 52±5*, 97±6 and 81±6* % of control, respectively).

pIC_{50} values for KN62 and PPADS were determined but were found to depend upon agonist concentration. Thus, against 0.5μM DbATP, pIC_{50} values for KN62 and PPADS were both 8.1±0.1, whereas against 8μM DbATP pIC_{50} values were 6.0±0.2 and 7.2±0.2, respectively.

Changing antagonist preincubation time did not significantly affect the results. For example 100nM KN62 inhibited responses to 4μM DbATP by 45±8, 51±8 and 53±6% when preincubation periods of 15, 30 or 60 min, respectively, were utilised. The effects of PPADS and KN62 were reversible following drug removal by dilution, centrifugation and resuspension of the cells. Thus, in the presence of 1μM KN62 or 1μM PPADS responses to 1μM DbATP were 4±2 % and -3±4% of control, respectively. Following washout of KN62 and PPADS responses to DbATP were 80±11% and 75±8% of control, respectively. Finally, PPADS but not KN62 was able to attenuate receptor inactivation produced by 100μM oxidised ATP (OxATP). Thus, in cells incubated with OxATP for 30mins and then washed, the response to 2μM DbATP was -3±1% of control whereas in cells pretreated with 1μM PPADS or 1μM KN62 for 15mins prior to OxATP treatment responses to 2μM DbATP following antagonist washout were 51±12 and -4±7%, respectively, of the response obtained in control cells.

These results confirm the ability of KN62 to antagonise $P2X_7$ receptor mediated cellular effects and also demonstrate that PPADS is a potent $P2X_7$ receptor antagonist. However, neither compound behaved competitively, although their effects were reversible. Their mechanisms probably differ since PPADS but not KN62 can attenuate receptor inactivation produced by OxATP.

Rassendren, F, Buell, G.N, Virginio, C. et al. (1997). J.Biol Chem. 272, 5482-5486.
Garget, C.E.,Wiley, J.S. (1997). Br. J. Pharmacol., 120, 1483-1490.

104P CHARACTERISATION OF ATP- AND LPS-INDUCED IL-1β RELEASE FROM THP-1 CELLS

C.B.A. Grahames, I.P. Chessell, A.D. Michel and P.P.A. Humphrey. Glaxo Institute of Applied Pharmacology, University of Cambridge, Department of Pharmacology, Tennis Court Road, Cambridge, CB2 1QJ.

Exogenous ATP can release IL-1β from activated immunocytes (Hoquist *et al.*, 1991). More recently, endogenous ATP release and subsequent $P2X_7$ purinoceptor activation has been implicated as the mechanism by which lipopolysaccharide (LPS) elicits release of IL-1β from microglial cells (Ferrari *et al.*, 1996). The aim of this study was to further characterise the ATP- induced IL-1β release from an activated human monocytic cell line (THP-1) and to investigate the involvement, if any, of ATP and $P2X_7$ purinoceptors in the LPS-induced IL-1β release in THP-1 cells.

THP-1 cells in suspension were treated with 0.5μM phorbol 12-myristate 13-acetate (PMA) for 3 h, washed three times in media and plated in 24 well plates at a density of 4 x 10^5 cells per well. 18 h later cells were activated with 10μgml^{-1} LPS for a further 18-24 h. Supernatants were removed and assayed for IL-1β. All experiments were carried out in media + 10% foetal calf serum at 37°C. Where appropriate (preincubation times in parentheses) oxidised ATP (OXATP) (120 min), KN-62 (30 min) and PPADS (30 min) were added prior to activation with LPS. In order to study ATP induced IL-1β release, cells were primed with PMA and LPS as described above and washed 3 times prior to a 30 min stimulation with 5mM ATP. Antagonists were preincubated prior to ATP stimulation for the times indicated above. Mature IL-1β and extracellular lactate dehydrogenase (LDH) in the supernatants were determined according to the assay kit suppliers' instructions (IL-1β EASIA-Medgenix and Cytotox-Promega, respectively). Extracellular ATP levels were measured using the firefly luciferase enzyme (Sigma).

LPS was found to release IL-1β in a concentration- and time-dependent manner; a concentration of 10μgml^{-1} for between 18-24h released 1429 ± 355 pgml^{-1} IL-1β compared to control levels of 41 ± 25 pgml^{-1}, and was used subsequently in all experiments. In PMA/LPS treated cells, ATP was shown to release IL-1β in both a concentration and time-dependent manner. The minimal effective ATP concentration was 1mM. Exposure of cells to 5mM ATP for 30 min released 1268 ± 470 pgml^{-1} IL-1β compared to non ATP-treated cells (34 ± 14pgml^{-1}) and was used routinely to stimulate IL-1β release from LPS primed cells. Exposure of cells to 5mM ATP under these experimental conditions for up to 6 h did not cause significant release of LDH. It was found that 1μM KN-62, or 100μM of either PPADS or OXATP significantly inhibited 5mM ATP-induced IL-1β release (table 1). However, these same compounds failed to significantly inhibit LPS-induced IL-1β release in these cells (table 1) and incubation with 1μM KN-62 caused a 31% increase in IL-1β release compared to control responses. Incubation with 0.4Uml^{-1} apyrase (an ATPase) failed to significantly inhibit LPS-induced IL-1β release (table 1). In separate experiments it was verified that all of the above compounds retained their activity after a 24 h incubation at 37°C.

We conclude that ATP release and subsequent $P2X_7$ purinoceptor activation is not involved in the LPS-induced IL-1β release in this cell type under these experimental conditions. Nonetheless the ability of the antagonists studied to inhibit both IL-1β release and pore formation by ATP (Michel *et al.*, this meeting) strongly suggests the involvement of the $P2X_7$ purinoceptor in ATP-induced IL-1β release from THP-1 cells.

Table 1: Effects of various compounds on both ATP and LPS-induced IL-1β release from THP-1 cells. NA- not applicable.

	% ATP stim (95% C.L.)	% LPS stim (95% C.L.)
100μM PPADS	10.2 (19.5-1.3)	92 (83-101)
1μM KN-62	16.1 (30.3-4.0)	131 (110-154)
100μM OXATP	33.8 (54.8-12.4)	84 (70-101)
0.4Uml^{-1} Apyrase	NA	83 (76.5-100)

Hoquist K.A., Nett M.A., Unanue E.R., Chaplin D.D. (1991). Proc. Nat. Acad. Sci. USA **88**, 8485-8489.
Ferrari D., Chiozzi P., Falzoni S. *et al.*, (1997). J. Exp. Med. **185**, 579-582.

105P MODULATION OF THE EXPRESSION OF THE HUMAN TYPE 1 α METABOTROPIC GLUTAMATE RECEPTOR IN CHINESE HAMSTER OVARY CELLS

E. Hermans, R.A.J. Challiss & S.R. Nahorski
Department of Cell Physiology & Pharmacology, University of Leicester, LE1 9HN

Metabotropic glutamate receptors (mGluR) constitute a broad family of G protein-coupled receptors for the excitatory amino acid glutamate. Recent studies have identified at least 8 subtypes of mGluR (mGluR1-8) that exhibit different biochemical and pharmacological properties (Conn & Pin, 1997). Receptor subtypes of the mGluR family constitute putative targets for drugs, but only a limited number of models are currently available for the study of signalling via these receptors.

Here, we report the stable expression of the human type 1α mGluR in CHO cells using an IPTG (isopropyl β-D-thiogalactopyranoside)-repressible expression system (LacSwitch II™). Treatment of the cells with IPTG resulted in a progressive increase in receptor expression, as detected by Western blot using a mGluR1α specific antiserum, or by assay of phosphoinositide hydrolysis induced by quisqualate (using cells radiolabelled for 48 h with [^{3}H]-inositol (Carruthers *et al.*, 1997)). Before treatment of the cells with IPTG, the signal observed in Western Blot was close to the detection threshold. Induction of the receptor expression by IPTG was time- and concentration-dependent. After 20 h incubation in the presence of 0.1 mM IPTG, a major immunoreactive signal was detected, and quisqualate (30 μM) was found to induce a 30-fold increase in phosphoinositide hydrolysis (30 min stimulation in the presence of 10 mM LiCl).

Under these conditions, the EC_{50} values for quisqualate, 1S,3R-ACPD, L-glutamate and (S)-3,5-DHPG inducing phosphoinositide hydrolysis were 0.40 ± 0.10; 35.2 ± 9.1; 5.47 ± 1.67 and 4.67 ± 1.16 μM respectively. The maximal response to 1S,3R-ACPD was 84% of the maximal response induced by quisqualate or glutamate, confirming the partial agonist activity of this compound at the mGluR1α receptor.

Using this model, it was possible to measure the consequence of altering receptor expression on the functional response to agonists. The cells were treated for 20 h with different concentrations of IPTG (2-100 μM), and the hydrolysis of phosphoinositides induced by quisqualate and 1S,3R-ACPD was measured. Analysis of responses of the cells to these two glutamate receptor agonists indicated that the increase in the level of receptor expression not only resulted in an increase in the maximum response, but also resulted in a progressive leftward shift of the concentration-response curves (see Table). These data indicate that the potencies of the agonists are dependent on the expression level of the receptor. Interestingly, the relative maximum response induced by 1S,3R-ACPD (calculated as percentage of the response obtained with quisqualate) on cells treated for 20 h with 100, 10 or 3 μM IPTG was 84, 72 and 37 %, respectively, indicating that the efficacy of this partial glutamate receptor agonist was also dependent on the expression level of the receptor.

This 'inducible' model system constitutes a useful tool for the study of biochemical and pharmacological properties of the human mGluR1α. In addition, the data presented indicate the importance of studying the functional coupling of metabotropic glutamate receptors in a model in which the expression level is tightly controlled.

Table : Agonist-induced inositol phosphate accumulation: EC_{50} values and % of maximal response (measured after induction with 0.1 mM IPTG)

IPTG	Quisqualate		1S,3R-ACPD	
	EC_{50} (μM)	% max	EC_{50} (μM)	% max
100 μM	0.40 ± 0.10 (8)	100	35.1 ± 9.1 (5)	100
30 μM	0.40 ± 0.04 (4)	98.7 ± 0.4	27.7 ± 2.5 (2)	106.7 ± 12.3
10 μM	0.89 ± 0.13 (5)	80.0 ± 0.3	62.4 ± 3.0 (2)	73.5 ± 3.1
3 μM	2.18 ± 0.18 (4)	15.4 ± 0.4	159 ± 3 (2)	9.2 ± 3.6

E. Hermans is a Visiting Research Fellow of the Wellcome Trust. We thank Glaxo-Wellcome for the gift of cDNA for mGluR1α.

Conn, P.J. & Pin, J.-P. (1997) *Ann. Rev. Pharmacol. Toxicol.* **37**, 205-237.
Carruthers, A.M., Challiss, R.A.J., Mistry, R. *et al.* (1997) *Mol. Pharmacol.* **52**, 406-414.

106P ENHANCED RECEPTOR-MEDIATED Ca^{2+} SGINALLING IN L-FIBROBLASTS OVEREXPRESSING TYPE-1 INOSITOL 1,4,5-TRISPHOSPHATE RECEPTORS

R.J. Davis, R.A.J. Challiss & S.R. Nahorski, Dept. of Cell Physiology & Pharmacology, University of Leicester, Maurice Shock Medical Sciences Building, P.O. Box 138, University Road, LEICESTER. LE1 9HN. UK.

We have recently characterised a mouse fibroblast cell-line that has been stably transfected with cDNA encoding the type-1 $InsP_3$-receptor. This L15 cell line expresses an 8-10 fold greater density of this intracellular receptor than cells (Lvec) transfected with an empty vector and displays enhanced Ca^{2+} mobilisation to Ins(1,4,5)P_3 and various synthetic analogues in permeabilised cells (Mackrill et al., 1996). In the present study we have examined the responses to the activation of cell-surface P2Y-receptors endogenously expressed on Lvec and L15 cells.

L-15 and L-vec cells were cultured as previously described (Mackrill et al., 1996). Ins(1,4,5)P_3 was assayed using a radioreceptor method (Challiss et al. 1990) and changes in $[Ca^{2+}]_i$ were measured by loading cells with Fura-2/AM (2μM 30 min) and assessing the ratiometric changes (λ_{ext} 340/380nM λ_{em} 510nM) in Fura-2 fluorescence. Measurements in cell populations were made in a Perkin Elmer LS50B fluorimeter and in single cells by imaging $[Ca^{2+}]_i$ (Applied Imaging Quanticell 700).

ATP and UTP dose-dependently stimulated a marked elevation of $[Ca^{2+}]_i$ in populations of Lvec and L15 cells. These agonists were equipotent and displayed similar sensitivity in both cells (pEC_{50} (M) values for UTP: Lvec, 5.36 ± 0.04; L15, 5.18 ± 0.12). However, the peak $[Ca^{2+}]_i$ responses to agonists were substantially ($p<0.01$) greater in the L15 cells. UTP also produced a dose-dependent elevation of Ins(1,4,5)P_3 that peaked at 30 s (basal: Lvec, 28 ± 1; L15, 30 ± 3; stimulated: Lvec 65 ± 3; L15, 70 ± 5 pmol mg^{-1} protein); responses were not significantly different in the L15 and Lvec cells. These data suggest that the P2Y-receptors are coupled to phospholipase C and that signalling proximal to the $InsP_3$- receptor is similar in both cell-lines. In order to investigate the marked difference in Ca^{2+} signalling between Lvec and L15 cells, a series of single cell imaging experiments were completed. Both cell-lines exhibited Ca^{2+} oscillations to sub-maximal concentrations of UTP but in agreement with the population studies the maximal Ca^{2+} responses were greater in the L15 cells. The threshold responses to agonist also revealed differences between the transfected cell-lines. Significant Ca^{2+} responses in Lvec cells were only seen at ≥300 nM UTP, whereas L15 cells displayed increased $[Ca^{2+}]_i$ at 100 nM.

These data demonstrate that L15 fibroblasts display enhanced Ca^{2+} signalling in response to UTP and ATP acting through cell-surface P2Y-receptors. Since activation of these receptors in L15 and Lvec cells results in a similar accumulation of Ins(1,4,5)P_3, we suggest that the enhanced Ca^{2+} response in L15 cells reflects the greater expression of type-1 $InsP_3$-receptors within this cell-line. These data provide the first evidence that altered $InsP_3$-receptor expression may influence cell-surface receptor-mediated Ca^{2+} signalling in cells.

This work was supported by the Wellcome Trust and BBSRC.

Challiss, R.A.J., Chilvers, E.R., Willcocks, A.L. et al. (1990) Biochem. J. **265**, 421-427.
Mackrill, J.J., Wilcox, R.A., Miyawaki, A. et al. (1996) Biochem. J. **318** 871-878.

107P AGONIST-MEDIATED SENSITISATION OF THE INS(1,4,5)P_3 RECEPTOR IN SH-SY5Y NEUROBLASTOMA CELLS

A.K. Martin, G.B. Willars & S.R. Nahorski, Dept. of Cell Physiology & Pharmacology, University of Leicester, Maurice Shock Medical Sciences Building, P.O. Box 138, University Road, LEICESTER. LE1 9HN. UK.

It has been long established that several receptor agonists can mobilise $[Ca^{2+}]_i$ by initiating a G-protein mediated activation of phospholipase C and generation of Ins(1,4,5)P_3. However, the relationship between Ins(1,4,5)P_3 accumulation and Ca^{2+} mobilisation is particularly complex, since the major species of Ins(1,4,5)P_3-sensitive release channels display multiple regulatory mechanisms particularly in response to changes in $[Ca^{2+}]_i$ (Mikoshiba, 1997). Here we have explored the possibility that receptor agonists may regulate the sensitivity of the Ins(1,4,5)P_3 activated channels independently of phosphoinositide hydrolysis and changes in $[Ca^{2+}]_i$.

SH-SY5Y cells were cultured as previously described (Willars & Nahorski, 1995) and $^{45}Ca^{2+}$ mobilisation was assessed in β-escin permeabilised cells following loading of stores as previously described (Strupish et al., 1988) and Ins(1,4,5)P_3 was assayed by a radioreceptor method. Exogenous Ins(1,4,5)P_3 dose-dependently released $^{45}Ca^{2+}$ from ionomycin-sensitive stores with a pEC_{50} (M) of 7.18 ± 0.03. Bradykinin alone failed to mobilise $^{45}Ca^{2+}$ at concentrations up to 10 μM but significantly ($p<0.05$) n=>3 enhanced Ins(1,4,5)P_3-evoked Ca^{2+} release (pEC_{50} (M) = 7.41 ± 0.02). This effect was reversed by the bradykinin antagonist HOE140, D-Arg^0-[Hyp^3, Thi^5, D-Tic^7, Oic^8] bradykinin (1μM) but not by the protein kinase C (PKC) inhibitor Ro 318220 (10μM). Methacholine alone dose-dependently mobilised $^{45}Ca^{2+}$ from ionomycin-sensitive stores with a pEC_{50} (M) of 5.49 ± 0.06 and this response was totally suppressed by heparin (100μg/ml) an inhibitor of Ins(1,4,5)P_3 induced Ca^{2+} release Methacholine induced $^{45}Ca^{2+}$ release was also suppressed by a combined pre-treatment of the cells with methacholine (1mM) and inhibition of PtdIns-4-kinase with wortmannin (10μM). This experimental protocol leads to a severe depletion of PtdIns(4,5)P_2 and suppression of Ins(1,4,5)P_3 accumulation (Willars et al. 1996). Under these conditions, exogenous Ins(1,4,5)P_3 mobilised $^{45}Ca^{2+}$ with a pEC_{50} (M) of 7.02 ± 0.1 and methacholine (1mM) significantly ($p<0.05$) potentiated this response (pEC_{50} (M) of 7.35 ± 0.01). This effect of methacholine was reversed by atropine (1μM) but not by Ro 318220(10μM) indicating a muscarinic receptor but not a PKC-mediated effect.

Finally, the sensitisation of Ins(1,4,5)P_3 induced $^{45}Ca^{2+}$ release by bradykinin and methacholine could be mimicked by GTPγS at concentrations (2μM) that failed to release $^{45}Ca^{2+}$ alone. These data may suggest the involvement of a G-protein in agonist-mediated enhanced Ins(1,4,5)P_3 mediated Ca^{2+} mobilisation. Overall these data indicate that cell surface receptors may be able to sensitise the Ins(1,4,5)P_3 receptor and/or release this site from a tonic inhibition. The resulting potentiation of Ca^{2+} mobilisation could represent a fundamental and physiologically important aspect of cell signalling.

This work is supported by the Wellcome Trust and BBSRC.

Mikoshiba K. (1997) Curr. Opin. Neurobiol. **7**, 339-345.
Strupish J., Cooke M., Potter B.V.L. et al. (1988) Biochem. J. **253**, 901-905
Willars G.B., Challiss R.A.J., Stuart J.A. et al. (1996) Biochem. J **316**, 905-913
Willars G.B. & Nahorski S.R. (1995) Brit. J. Pharmacol. **114**, 1133 1142

108P BIS-DIPHOSPHOINOSITOL TETRAKISPHOSPHATE (IP_8) LEVELS ARE MEDIATED BY A CYCLIC AMP-DEPENDENT, PROTEIN KINASE A-INDEPENDENT PATHWAY IN SMOOTH MUSCLE CELLS

S.T Safrany and S.B. Shears. Inositide Signaling Section, Laboratory of Signal Transduction, NIEHS, NIH, R.T.P., NC 27709, USA.

Bis-diphosphoinositol tetrakisphosphate (IP_8) and its precursor, diphosphoinositol pentakisphosphate (IP_7) are the most highly phosphorylated members of the inositide family yet described. They are formed from sequential phosphorylation of inositol hexakisphosphate (IP_6) (Shears *et al.*, 1995). The high energy potential of the β-phosphate identifies these molecules as excellent candidates for driving energy-demanding processes and/or transphosphorylation reactions (Voglmaier *et al.*, 1996).

We have used a DDT_1 MF-2 Syrian hamster vas deferens smooth muscle cell line to determine a mechanism by which G-protein coupled receptor activation causes a decrease in cellular IP_8 levels to 40-50% of control levels.

DDT_1 MF-2 cells were prelabelled with 50μCi/ml [^{3}H]-inositol for six days. Monolayers of cells were washed in Krebs-Henseleit buffer (pH 7.4) and equilibrated for 3 hours before commencement of experiments. Cells were treated with agonists for 2-90 minutes and incubations were quenched by the addition of ice-cold 0.6M PCA containing 0.2mg/ml IP_6. Samples were neutralised by the addition of 2M K_2CO_3 5mM EDTA. Inositol phosphates were then separated using a Partisphere hplc column.

Isoprenaline (1μM), acting on β_2-adrenoceptors caused a time- and dose-dependent decrease in cellular IP_8.

The decrease in IP_8 was observed within 5 minutes and was maximal by 30 minutes. Dose-response relationships, obtained at 30 minutes, identified that isoprenaline was very potent with EC_{50} 0.43 (0.1-2.0) nM {Mean (95% confidence limits), n=5}, reducing IP_8 to 42 ± 4% of control.

The effects of isoprenaline were reproduced by the phosphodiesterase inhibitor 3-isobutyl 1-methylxanthine, suggesting a role for cyclic nucleotides. Dibutyryl cyclic AMP {EC_{50} 15(4-53)μM, n=5} and dibutyryl cyclic GMP {EC_{50} 8(1-68)μM, n=4} also caused a decrease in IP_8 levels to 50 ± 5% and 58 ± 7% of control respectively.

The effects of isoprenaline, dibutyryl cyclic AMP and dibutyryl cyclic GMP were not affected by H-89 (1μM), HA1077 (30μM), Rp-CPT-cyclic AMPS (100μM) or Rp-CPT-cyclic GMPS (100μM), ruling out the role of protein kinase A and protein kinase G. The role of cyclic nucleotide-gated cation channels has also been excluded.

These observations show, for the first time, regulation of IP_8, and identify the mechanism as a novel cyclic nucleotide-mediated pathway. We anticipate these results to aid in the identification of the physiological role of IP_8

Shears, S.B. *et al.*, (1995) J. Biol. Chem. 270, 10489-10497.
Voglmaier, S.M. *et al.*, (1996) Proc. Natl. Acad. Sci. USA 93, 4305-4310.

109P [^{125}I]TYR^3 OCTREOTIDE LABELS HUMAN SOMATOSTATIN sst_2 AND sst_5 RECEPTORS EXPRESSED IN CCL39 CELLS

S. Siehler, K. Seuwen & D. Hoyer Preclinical Research, Novartis Pharma AG, S-386/745, 4002 Basel, Switzerland

There are two families of receptors for somatostatin (SRIF, somatotropin release inhibiting factor), SRIF-1 (sst2, sst3, sst5) with high or very high affinity for octreotide (SMS 201-995, Sandostatine), seglitide (MK 678) and somatuline (BIM 23014) and SRIF-2 (sst1, sst4) with very low affinity for small analogues (Hoyer *et al*, 1995). [^{125}I]-Tyr^3-octreotide has long been assumed to label exclusively sst2 receptors. However, we show here that human somatostatin sst_2 and sst_5 receptors (Yamada *et al.*, 1993; Panetta *et al.*, 1994) stably expressed in CCL39 hamster lung fibroblast cells bound [^{125}I]-Tyr^3-octreotide with high affinity and in a saturable manner (pK_d = 9.89±0.02; B_{max} = 210±10 fmol/mg protein and pK_d = 9.64±0.04; B_{max} = 920±170 fmol/mg, respectively).

The pharmacological profile of sst_2 and sst_5 sites labelled with [^{125}I]-Tyr^3-octreotide was established for both receptors in radioligand competition studies using standard SRIF analogues (for abbreviations see Hoyer *et al*, 1994): (pK_d-values for sst_2 and sst_5, respectively) SRIF14 (10.01±0.04, 9.87±0.24), SRIF28 (9.99±0.02, 10.30±0.25), cortistatin14 (9.00±0.09, 9.65±0.22), seglitide (9.81±0.13, 10.18±0.22), CGP23996 (8.95±0.07, 8.68±0.20), octreotide (9.10±0.07, 9.48±0.11), cycloantagonist SA (5.77±0.05, 8.25±0.17), RC160 (9.50±0.16, 9.13±0.35), L362.855 (8.79±0.06, 9.17±0.10), L363.301 (8.39±0.08, 9.51±0.14), BIM23014 = somatuline (9.55±0.03, 9.31±0.10), BIM23030 (7.94±0.22, 7.45±0.18), BIM23052 (8.55±0.01, 9.28±0.35), BIM23056 (6.38±0.11, 8.32±0.17).

It is striking that both profiles are very similar and that molecules classically known as sst2 receptor selective (e.g. seglitide, octreotide, RC 160, somatuline) show very high affinity for human sst5 receptors. Differences with published data may relate to the use of a distinct radioligand, e.g. [^{125}I]-Tyr^3-octreotide instead of [^{125}I]-CGP23996 or [^{125}I]-(Leu^8, D-Trp^{22}, Tyr^{25})-SRIF28, to label human sst5 receptors.

It is established that Octreotide and a number of short chain SRIF mimics inhibit tumour cell growth. This antiproliferative effect may not only be mediated by sst_2, but also by sst5 receptors. Interestingly cortistatin14 (a putative neuropeptide very similar to SRIF but produced by a separate gene) bound with similar high affinity comparable to SRIF14/28 to human sst2 and sst_5 receptors, suggesting cortistatin and somatostatin to share targets.

Finally, one may anticipate that Octreoscan® used in vivo to visualise SRIF receptor bearing tumours, may also recognise sst5 receptors in addition to sst2 receptors.

Hoyer, D., Lübbert, H. and Bruns, C. Naunyn-Schmiedeberg's Arch. Pharmacol. 1994, 350:441-453
Hoyer, D., Bell, G.I., Berelowitz, M. *et al*, TiPS, 1995, 16: 86-88
Panetta, R., Greenwood, M.T., Warszynska, A. *et al.*, Mol.Pharmacol. 1994: 45:417-427.
Yamada, Y., Kagimoto, S., Kubota, A. *et al.*, Biochem. Biophys. Res. Comm. 1993, 195:844-852.

110P SOMATOSTATIN-INDUCED INCREASES IN EXTRACELLULAR ACIDIFICATION RATES, ACTIVATION OF MAP-KINASE AND INHIBITION OF ADENYLYL CYCLASE IN CHO-K1 CELLS EXPRESSING RAT sst_{2A} AND sst_{2B} RECEPTORS

M. Schindler, A.M. Carruthers, W. Feniuk and P.P.A. Humphrey. Glaxo Institute of Applied Pharmacology, University of Cambridge, Tennis Court Road, Cambridge, CB2 1QJ.

Two splice variants of the mouse sst_2 receptor exist, sst_{2a} and sst_{2b} differing in the composition of the intracellular carboxy-terminus (Vanetti et al., 1992). The two isoforms have been claimed to differ in their coupling to adenylyl cyclase (Reisine et al., 1993). Following the cloning of a rat sst_{2b} receptor (Kidd et al., this meeting), we have compared the receptor-G protein coupling of this receptor with that of the rat sst_{2a} expressed in CHO-K1 cells.

Somatostatin (SRIF)-induced increases in extracellular acidification rates (EAR) were measured by microphysiometry as previously described (Castro et al., 1996). SRIF-induced activation of p42 and p44 MAP kinase (ERK2 and ERK1) was measured using a peptide phosphorylation assay (Amtrak, Amersham). SRIF-induced inhibition of forskolin (10μM)-induced increases in cAMP were measured as previously described (Williams et al., 1996) using a radioligand binding assay (Brown et al., 1971). In some studies, cells were pre-treated with 100ng/ml pertussis toxin (PTX) 18h prior to experimentation. All values shown are mean ± se mean from 3-5 experiments.

Using microphysiometry, the basal rates of EAR were 100-300μV/s (0.1-0.3 pH unit/min). SRIF caused concentration dependent increases in EAR in CHO-K1 cells expressing either rat sst_{2a} or sst_{2b} receptors (pEC_{50} values: 9.0±0.2 and 9.9±0.1; maximal effect: 180±14 and 161±8μV/s respectively). PTX pretreatment caused a rightward displacement of the SRIF concentration effect curves (pEC_{50} values: 8.3±0.2 and 8.4±0.2; maximal effect: 155±17 and 109±10 μV/s respectively). Maximal responses to SRIF were transient (<10 min duration) in control cells but were more sustained (up to 30min) after PTX treatment. SRIF also concentration-dependently activated MAP-kinase in CHO-K1 cells expressing the rat sst_{2a} or sst_{2b} receptors. SRIF was about 3 times more potent in the CHO-K1 cells expressing the rat sst_{2a} (pEC_{50} 9.1±0.1) than the rat sst_{2b} receptors (pEC_{50} 8.6±0.1). The maximum stimulation of MAP-kinase by SRIF in the former cells was approximately 200% of that obtained in the latter. Following pretreatment with PTX, SRIF (10pM-100nM) had little effect on MAP-kinase activity in either cell type.

Incubation with forskolin (10μM) for 10 min caused an approximate 40 fold increase in basal cAMP accumulation. Forskolin-induced increases in cAMP accumulation were inhibited by SRIF (1pM-10nM) in a concentration dependent manner (rat sst_{2a}, pEC_{50} 10.6 ± 0.2: rat sst_{2b}, pEC_{50} 10.6 ± 0.2). Maximum inhibitions were 94.8 ± 1.4% and 74.5 ± 7.5%, respectively. Higher concentrations of SRIF (30nM-1μM) caused smaller inhibitions of forskolin activated adenylyl cyclase, resulting in bell shaped concentration-effect curves. Pretreatment with PTX abolished the inhibitory effect of SRIF which caused increases in cAMP accumulation above the level observed with forskolin (224 ± 27% and 191 ± 24% for sst_{2a} and sst_{2b} respectively, at a concentration of 10μM SRIF).

The results from the present study demonstrate the effective coupling of both the rat recombinant sst_{2a} and sst_{2b} receptors to a number of different transduction systems. Both receptors appear to couple to $G_{i/o}$ as well as other G-proteins since both PTX-sensitive and -insensitive components were observed in the microphysiometry and adenylyl cyclase studies.

Brown, B. et al., (1971). *Biochem. J.*, **121**, 561-562.
Castro, S. et al., (1996). *Br. J. Pharmacol.*, **117**, 639-646.
Reisine, T. et al., (1993). *Mol. Pharmacol.*, **44**, 1008-1015.
Vanetti, M. et al., (1992). *FEBS Lett.*, **311**, 290-294.
Williams, A.J. et al., (1996). *Br. J. Pharmacol.*, **119**, 11P.

111P FUNCTIONAL STUDIES WITH THE NOVEL SOMATOSTATIN (SRIF) sst_2 RECEPTOR BLOCKING DRUG AcNH-4-NO_2-Phe-c[D-Cys-Tyr-D-Trp-Lys-Thr-Cys]-Tyr-NH_2 (CYANAMID 154806)

W. Feniuk, E.M. Jarvie, J. Luo, J.A. Humphrey and P.P.A. Humphrey. Glaxo Institute of Applied Pharmacology, University of Cambridge, Department of Pharmacology, Tennis Court Rd., Cambridge, CB2 1QJ

The characterisation and physiological significance of SRIF receptor types has been hampered by the lack of potent and selective SRIF receptor blocking drugs. Recently, Bass and colleagues, (1996) described the antagonistic activity of the cyclic octapeptide, Cyanamid 154806 on SRIF-induced inhibition of cAMP formation in cells transfected with the rat sst_2 and rat sst_5 receptor subtypes. We have now investigated the selectivity of the L-Tyr^8 isomer of Cyanamid 154806 in radioligand binding studies in CHO-K1 cell membranes expressing human recombinant sst_1-sst_5 receptors as well as rat recombinant sst_{2a} and sst_{2b} receptors (Schindler et al., this meeting). The effect of L-Tyr^8-CYN 154806 has also been studied on tissues, namely, SRIF-induced inhibition of neurogenic contractions in rat vas deferens, guinea-pig ileum and guinea-pig vas deferens.

In radioligand binding studies, membranes (1-3μg protein) from CHO-K1 cells expressing each recombinant SRIF-receptor subtype were incubated with 0.03nM [^{125}I]-Tyr^{11}-SRIF for 90 min in the absence and presence of increasing concentrations of L-Tyr^8-CYN 154806 at room temperature. Non specific binding was defined by 1μM SRIF. Analysis of the competition curves were made assuming the ligand bound to single site and pIC_{50} values determined using Graph Pad Prism. The antagonistic effect of L-Tyr^8-CYN 154806 on SRIF-, or SRIF-28-induced inhibition of neurogenic contractions of guinea pig isolated ileum and guinea pig vas deferens were determined as previously described (Feniuk et al., 1995) as was the effect on SRIF-induced inhibition of neurogenic (0.1Hz, 0.5ms, 700mA) contractions of rat vas deferens. The antagonist contact time was 30min. All values are mean ± se mean or geometric mean (range) from at least 4 experiments.

L-Tyr^8-CYN 154806 inhibited (pIC_{50}) specific [^{125}I]-Tyr^{11}-SRIF binding to CHO-K1 cell membranes expressing h sst_1 (5.41±0.04), h sst_2 (8.58±0.07), h sst_3 (6.07±0.04), h sst_4 (5.76±0.09), h sst_5 (6.48±0.09), r sst_{2a} (8.35±0.19) and r sst_{2b} (8.10±0.10) receptors.

SRIF caused a concentration dependent inhibition of neurogenic contraction in rat isolated vas deferens [EC_{50} 34(27-56)nM]. L-Tyr^8-CYN 154806 (0.1, 0.3 and 1.0μM) displaced the SRIF concentration-effect curve to the right [SRIF concentration-ratios 6.7(5.5-9.3), 19.5(14.4-32.8) and 67.9(45.6-129.6) respectively] with no depression of the maximum response giving a meaned pK_B estimate of 7.79±0.05. SRIF [EC_{50} 43(35-50)nM also inhibited neurogenic contraction of guinea-pig ileum and these responses were also antagonised by L-Tyr^8-CYN 154806 (0.1 and 1.0μM). The SRIF concentration ratios were 5.0(3.6-8.8) and 25.8(11.4-96.6) respectively giving a meaned pK_B estimate of 7.49±0.11. L-Tyr^8-CYN 154806 (1μM) had no effect on the inhibitory action of the μ-agonist DAMGO in either the rat vas deferens or guinea-pig ileum [concentration ratios 0.81(0.50-1.15) and 0.96(0.91-1.10)] respectively. SRIF-28 [EC_{50} 44(15-80)nM] caused concentration dependent inhibition of neurogenic contraction in the guinea-pig vas deferens, L-Tyr^8-CYN 154806 (1μM) had no effect on this response [concentration-ratio 1.9(1.2-3.0)].

The results show that L-Tyr^8-CYN 154806 is a highly selective ligand at somatostatin sst_2 receptors. Functional studies in guinea-pig ileum and rat vas deferens have demonstrated its antagonistic activity and the data are consistent with the view that sst_2 receptors mediate inhibition of neurogenic contraction. The receptor in the guinea-pig vas deferens is different and may be an sst_5 receptor (Feniuk et al.,1995).

Bass, R.T. et al., (1996). *Mol. Pharmacol.*, **50**, 709-715.
Feniuk, W. et al., (1995). *Br. J. Pharmacol.*, **115**, 975-980.

112P REGIONAL DISTRIBUTION OF 5-HT_{2C} RECEPTOR mRNA IN HUMAN TISSUES USING REAL TIME, QUANTITATIVE SEQUENCE DETECTION

G.S. Baxter, R.A. Coleman, A. Miah, O.E. Murphy & J.E. Carey Pharmagene Laboratories PLC, 2A Orchard Road, Royston, Herts. SG8 5HD.

5-HT_{2C} receptors are thought to be expressed exclusively in the central nervous system (CNS) (Hoyer *et al.*, 1993). We have now examined the expression of 5-HT_{2C} mRNA in human peripheral tissues using the ABI PRISM™ 7700 sequence detection system (Carey *et al.*, 1997).

A pair of primers and a TaqMan probe were designed to amplify a 91 base pair fragment of the third intra-cytoplasmic loop of the human 5-HT_{2C} nucleotide sequence (forward primer 5' GGAACCGCCTGGACTAA GTCT-3', reverse primer 5' TCTGGTCTTGGTTAGGGTTTGC-3', probe 5' TTCTCTTCCTCGGCCGTATTCCTCTTGT-3'). A primer / probe set for human β-actin was also used to assess RNA integrity in each sample (*see* Carey *et al.*, (1997). Total RNA was extracted from a range of human peripheral tissues as described by Murphy *et al.*, (1997). To benchmark CNS versus peripheral expression levels, a sample of human caudate was also used. 500ng of total RNA from each tissue was annealed to 1.25 pmol of each of the reverse primers for 5-HT_{2C} and ß-actin and the cDNA synthesis step was essentially as described by Carey et al., (1997) but, in addition, 250ng of total RNA from each tissue was subjected to the annealing and cDNA synthesis steps in the absence of reverse transcriptase. This 'no amplification control' (NAC) allowed any contaminating DNA contribution to the 5-HT_{2C} Cn to be subtracted. 250ng of reverse transcribed total RNA was amplified to identify either 5-HT_{2C} or β-actin molecules nucleotide sequences. The NAC was also subject to 5HT_{2C} amplification. The final reaction conditions for 5-HT_{2C} nucleotide sequence detection were; forward primer (50nM), reverse primer (900nM), probe (250nM), 6% glycerol, TaqMan buffer A (Perkin Elmer), $MgCl_2$ (7.5mM), 200μM each of dATP, dGTP, dCTP, dTTP and 1.25 units of AmpliTaq Gold (Perkin Elmer). The reaction conditions for β-actin were identical except that a probe concentration of 150nM was used. Standard curves were constructed for both the 5-HT_{2C} and actin sequences using 1,000-20,000 genome equivalents of sheared human DNA. PCR reactions were carried out in duplicate under identical conditions to those described above.

5-HT_{2C} and β-actin mRNA transcripts were detected in both CNS and peripheral tissues (Table 1). The highest level of 5-HT_{2C} mRNA expression (>10,000 copies) was detected in pulmonary blood vessels and was approximately 5-fold higher than that observed in human caudate.

Table 1. Threshold cycles (Ct) and copy number (Cn) for 5-HT_{2C} and β-actin mRNA transcripts in human tissues. Cn values for 5-HT_{2C} are corrected by subtracting Cn values calculated for the NAC.

TISSUE	5-HT_{2C} Ct	5-HT_{2C} log Cn-NAC	actin Ct	actin log Cn
pulmonary vessels	22.1	4.17	26.7	3.67
trachea	23.5	3.86	23.5	4.31
caudate	25.0	3.50	19.9	4.15
gall bladder	25.1	3.43	24.6	4.15
placenta	25.2	3.32	19.1	5.39
kidney medulla	26.9	2.96	29.7	3.01
colon muscle	26.8	3.11	25.9	3.74
lymph node	27.1	2.80	25.0	3.94
aorta	27.5	2.61	21.3	4.33
liver	28.0	2.42	16.9	5.40
stomach mucosa	29.3	2.55	24.6	4.12
ileum muscle	29.3	2.29	24.4	4.10
cerebral vessels	28.4	2.20	21.0	4.46
foreskin	29.4	2.05	26.0	3.44

These data indicate that 5-HT_{2C} mRNA is present in peripheral tissues and suggests that 5-HT_{2C} receptors may be involved in peripheral function.

References

Carey, J.E., Miah, A., Murphy, O.E. *et al.*, (1997) *Br. J. Pharmacol* (this meeting)
Murphy O.E., Carey, J.E., Miah, A. *et al.*, (1997) *Br. J. Pharmacol* (this meeting)
Hoyer, D. *et al.*, (1993) *Pharmacol. Rev.*, **46**, 157.

113P QUANTIFICATION OF mRNA TRANSCRIPT COPY NUMBER USING THE ABI PRISM™ SEQUENCE DETECTION SYSTEM

J.E.Carey, A.Miah, O.E.Murphy, R.A.Coleman & G.S.Baxter. Pharmagene PLC, 2A Orchard Road, Royston, Herts. SG8 5HD.

The detection of mRNA in tissues and cells can provide clues as to the expression and biological function of encoded proteins. However, most of the currently available detection methods rely on analysis at endpoint, are labour intensive and do not allow accurate calculation of mRNA copy numbers. We describe the development of a quantitative, real time detection protocol for mRNA transcripts using the ABI PRISM™ 7700 sequence detection system (Heid *et al.*, 1996).

A pair of primers and a TaqMan probe were designed and synthesised to amplify and detect a 350 base pair fragment of the human β-actin nucleotide sequence (forward primer 5' CAGCGGAACCGCTCATTG CCAATGG-3', reverse primer 5' TCACCCACACTGTGCCCATCTA CGA-3', probe 5' ATGCCCTCCCCCATGCCATCCTGCGT-3'). In previous studies, in the absence of reverse transcriptase, this primer / probe set has been shown to detect little or no target sequence in total RNA samples (data not shown). Total RNA was extracted from human tissues as described by Murphy *et al.*, (1997). 250ng of total RNA from each tissue was annealed to 1.25 pmole of the reverse primer for actin by heating to 72°C and cooling slowly to 55°C in the presence of KCl (50mM), Tris HCl (10mM, pH8.3) and $MgCl_2$ (5mM). The cDNA synthesis step of 48°C for 30mins, 90°C for 5mins was carried out in KCl (50mM), Tris HCl (10mM, pH8.3), $MgCl_2$ (5mM), dATP, dGTP, dTTP, dCTP (each at 1mM) and MuLV reverse transcriptase (12.5 units) (Perkin Elmer). PCR amplification was carried out on the ABI PRISM™ 7700 sequence detection system. An initial AmpliTaq Gold (Perkin Elmer) activation step, 94°C for 12 min, was followed by 45 cycles of PCR at 94°C for 15 secs, 60°C for 1 min with minimum ramp time. 250ng of reverse transcribed total RNA was amplified to identify actin nucleotide sequences. The final reaction conditions for nucleotide sequence detection were; forward primer (50nM), reverse primer (900nM), probe (150nM), 6% glycerol, TaqMan buffer A (Perkin Elmer), $MgCl_2$ (7.5mM), dATP, dGTP, dCTP, dTTP (each at 200μM) and 1.25 units of AmpliTaq Gold. A standard curve for actin nucleotide sequence detection was constructed using 1,000-20,000 genome equivalents of sheared human DNA. PCR reactions were carried out in duplicate under identical conditions to those described above.

Table 1. Mean threshold cycle (Ct) and mean $\log_{10}$ transcript copy number (Cn) for actin nucleotide sequence detection in human tissues. PCR reactions were carried out on identical total RNA samples.

Tissue	Ct ± s.e.m.	Log Cn ± s.e.m.	n
Oesophagus	17.6 ± 0.79	5.93 ± 0.19	6
Caudate	21.7 ± 1.42	5.21 ± 0.26	6
Ileum	22.0 ± 0.51	4.85 ± 0.21	6
Basal artery	21.9 ± 1.10	4.66 ± 0.25	6
Colon	24.5 ± 0.99	3.89 ± 0.06	6
Prostate	26.6 ± 1.31	3.88 ± 0.09	6

The PCR cycle for detection of a threshold fluorescent signal (Ct) in human tissue samples ranged from 17.6 to 26.6 (Table 1) indicating the presence of actin mRNA nucleotide sequence in high abundance in all tissues tested. The starting copy number (Cn) for actin mRNA was calculated by reference to the standard curves and ranged from over 7000 in prostate to almost 1,000,000 in oesophagus. In each case, the variability over 6 separate PCR runs was low.

These data indicate that quantitative PCR using the ABI PRISM™ 7700 permits robust and reproducible detection and quantification of target mRNA nucleotide sequences. These data also indicate that the abundance of actin mRNA detected within identical quantities of total RNA differ by over 100-fold between tissues. This suggests that actin does not represent a useful means of normalising samples in this system. Nevertheless, the use of actin mRNA as a marker of transcript integrity remains a valid approach (Murphy *et al.*, 1997)

Heid, C.A., Stevens, J. Livak, K.J. *et al* (1996) *Genome Research*, 6; 986-994

Murphy O.E., Carey, J.E., Miah A., *et al.*, *Br. J. Pharmacol* (this meeting)

114P ASSESSMENT OF SAMPLE QUALITY OF TOTAL RNA FOR mRNA EXPRESSION STUDIES

O.E. Murphy, J.E. Carey, A. Miah, R.A. Coleman & G.S. Baxter Pharmagene PLC, 2A Orchard Road, Royston, Herts., SG8 5HD.

New techniques for quantifying mRNA levels in tissue samples can provide important markers of encoded protein function (Carey *et al.*, 1997). However, the value of such techniques can be eroded by a failure to account for degradation of mRNA and contamination of samples during the extraction process. The ability to assess RNA sample quality is therefore an essential prerequisite for the generation of robust gene expression data.

Samples of human liver, hypothalamus and lung blood vessels were obtained from multiple donors with variable post mortem delay. Tissues (<0.5 cm^3) were snap frozen in liquid nitrogen and stored at -80°C until use. For RNA extraction, each tissue sample was homogenised in TRIzol reagent for 150 sec using a high speed Waring blender. Total RNA was extracted from the homogenate as described by Verhofstede *et al.* (1996) and dissolved in up to 50μl of nuclease-free H_2O.

The yield of RNA extracted from each tissue was established using an A_{260} spectrophotometer reading and the final concentration of each sample adjusted to give a 1μg μl^{-1} stock solution. Using these stock solutions, the quality of total RNA was evaluated by establishing the presence of 18s and 28s ribosomal RNA bands on a denaturing agarose gel and of β-actin mRNA copies (Cn) using the ABI PRISM™7700 sequence detection system (Carey *et al.*, 1997). Contamination with protein and/or phenol (used in the extraction process) was established through measurement of A_{260} / A_{280} ratios where a value of < 1.7 indicates contamination.

Tissues produced a variable yield of total RNA. While hypothalamus and lung blood vessel yields were similar, those from liver samples were up to 10-fold higher. In every sample, 18s and 28s bands were present, and all samples had a A_{260} / A_{280} ratio of 1.7 or greater, indicating the presence of intact RNA with little or no contamination. However, it was not possible to detect β-actin mRNA in two of the hypothalamus samples, suggesting possible mRNA degradation and or the presence of an inhibitor of the RT-PCR process.

Table 1. Quality control parameters for assessment of RNA integrity and sample contamination

Human tissue (pm delay)	RNA yield μg mg^{-1} tissue	RNA integrity 18s bands	RNA integrity 28s bands	RNA integrity log β-actin (Cn)	A_{260} / A_{280} ratio
Liver (<48h)	1.45	+	+	4.47	1.82
Liver (3h)	3.30	+	+	4.82	1.77
Liver (2h)	0.464	+	+	5.35	1.80
Hypothalamus (7h)	0.322	+	+	2.69	1.82
Hypothalamus (3h)	0.407	+	+	No actin	1.92
Hypothalamus (4h)	0.173	+	+	No actin	2.01
Lung vessels (<6h)	0.127	+	+	3.86	1.82
Lung vessels (7h)	0.148	+	+	4.24	1.81
Lung vessels (7h)	0.291	+	+	4.51	1.70

These data suggest that assessment of ribosomal RNA and spectrophotometer ratios alone are not sufficient to determine the suitability of RNA samples for quantitative gene expression studies. A more complete assessment of suitability can be provided by including direct measurement of a specific mRNA such as that encoding β-actin (Carey *et al.*, 1997).

Carey, J.E. Miah, A. Murphy, O.E. *et al.*, *Br. J. Pharmacol* (this meeting)

Verhofstede, C., Fransen, K., Marissens, D. *et al* (1996) *J Virol methods*, 60, 155 - 159

We gratefully acknowledge the Netherlands Brain Bank and IIAM for provision of human tissue samples.

115P EFFECT OF INTERLEUKIN-1β ON CHOLINERGIC CONTRACTIONS OF THE RAT GASTRIC FUNDUS

T.G. Moreels, J.G. De Man, B.Y. De Winter, A.G. Herman & P.A. Pelckmans. Div. of Gastroenterology and Pharmacology, University of Antwerp (UIA), Universiteitsplein 1, B-2160 Wilrijk, Belgium.

Recently it has been shown that the majority of patients with ileocolonic Crohn's disease (CD) have focally enhanced gastritis which is not Helicobacter pylori-induced (Oberhuber *et al.*, 1997). Inflammation of the stomach may induce upper gastrointestinal motility disturbances. Since interleukin-1β (IL1β) is an important inflammatory mediator in CD, we studied the effect of the human recombinant IL1β on the electrical and pharmacological properties of the gastric fundus from male Wistar rats (250-350g). After removal of the mucosa, longitudinal muscle strips were mounted in organ baths filled with aerated Krebs-Ringer solution for isometric tension recording. The strips were placed at their optimal length-tension relationship using carbachol (10^{-8}M). Cumulative dose and frequency response curves were obtained for acetylcholine (ACh, 10^{-9}-$3x10^{-7}$M) and electrical stimulation (ES, 0.25-8Hz, 1ms pulse duration, 10s pulse trains) respectively. Contractions were expressed as the percentage of a 50mM KCl contraction. Results are shown as the mean±s.e.m. for the number of experiments indicated. After exposure of the strips to increasing concentrations of IL1β, the contractions induced by 2Hz were recorded at different time intervals. The contractions were dose and time dependently increased by IL1β. In control conditions the ES-induced contraction was 57.3±5.1% (n=8). After 60 minutes of incubation with 0.1ng/ml, 1ng/ml and 10ng/ml IL1β the contractions were 63.8±4.2% (P=0.54, n=8), 71.4±3.7% (P=0.054, n=8) and 78.7±3.1% (P=0.003, n=8) respectively. In the following experiments the strips were incubated for 60 minutes with 10ng/ml IL1β. The ratio of the KCl-induced contraction in grams to the weight of the strips was not significantly altered by the exposure to IL1β. Both ES- and ACh-induced contractions were significantly increased by IL1β (Table 1). The cyclo-oxygenase inhibitor indomethacin (indo, $3x10^{-6}$M) reversed the action of IL1β, whereas indomethacin alone had no effect (Table 1).

Table 1: Effect of IL1β and indo on ES- and ACh-induced contractions

		control	IL1β	IL1β+indo	indo
ES	0.25Hz	41.9±8.5	76.2±4.8*	33.0±9.0	25.1±6.8
	8Hz	85.5±3.5	108.3±6.6*	85.6±5.2	75.5±3.5
ACh	10^{-9}M	24.7±5.9	51.2±7.7*	11.8±7.0	13.3±5.7
	$3x10^{-7}$M	98.4±3.1	117.1±3.3*	99.2±4.6	95.3±2.0

**, P≤0.05, vs. other groups; one-way ANOVA followed by Student-Newman-Keuls test, n=8.*

The IL1β-induced stimulatory effect on the ACh-induced contractions was reversed by the neurotoxin tetrodotoxin (TTX, 10^{-6}M), two minutes before adding ACh (Table 2). TTX alone had no effect (Table 2).

Table 2: Effect of IL1β and TTX on ACh-induced contractions

		control	IL1β	IL1β+TTX	TTX
ACh	10^{-9}M	12.2±4.5	43.0±5.2*	22.9±5.8	14.9±3.2
	$3x10^{-7}$M	96.8±4.6	109.4±3.8*	92.8±3.5	91.5±2.4

**, P≤0.05, vs. other groups; one-way ANOVA followed by Student-Newman-Keuls test, n=8.*

In conclusion, our results demonstrate that the inflammatory mediator IL1β stimulates the ES- and ACh-induced contractions of longitudinal muscle strips of the rat gastric fundus. This effect is mediated through an increased release of prostanoids since indomethacin reversed the action of IL1β. Finally, the action of IL1β is neurally mediated since TTX reversed the effect of IL1β. These results suggest that inflammation can indeed cause disturbances in upper gastrointestinal motility in rats.

Oberhuber, G. *et al.*, (1997) *Gastroenterology*, 112, 698-706.

116P EFFECT OF ASCORBATE ON RELAXATIONS TO S-NITROSOTHIOLS AND ON THE NITRERGIC NEUROTRANSMITTER IN THE RAT GASTRIC FUNDUS

J.G. De Man, B.Y. De Winter, T.G. Moreels, A.G. Herman & P.A. Pelckmans. Div. of Gastroenterology and Pharmacology, University of Antwerp (UIA), Universiteitsplein 1, B-2610 Wilrijk, Belgium

The exact nature of the nitrergic neurotransmitter released from non-adrenergic non-cholinergic (NANC) nerves is still debated. As responses to authentic nitric oxide (NO) but not those to nitrergic stimulation are inhibited by superoxide generators, it was suggested that the nitrergic neurotransmitter is not free NO but an NO-releasing substance such as an S-nitrosothiol. Alternatively, tissue antioxidants such as ascorbate might protect the nitrergic neurotransmitter from breakdown by superoxides (Martin et al., 1994, Gibson et al., 1996). In this study, we investigated the effect of ascorbate on relaxations to nitrergic stimulation and on those to S-nitrosothiols.

Longitudinal muscle strips of the gastric fundus from male Wistar rats were mounted in organ baths, filled with Krebs-Ringer solution, and precontracted with prostaglandin $F_{2\alpha}$ (0.3 μM). Experiments were performed in the presence of atropine (1 μM) and guanethidine (3 μM). Results are expressed as mean±s.e.m. Statistical significance was calculated by Student's t test for the number of rats indicated. P<0.05 was considered as statistically different from control.

The S-nitrosothiols S-nitrosoglutathione (GSNO, 0.1 μM) and S-nitrosocysteine (CysNO, 10 nM) relaxed the rat gastric fundus. Incubation of the tissue with ascorbate (1-3 μM) concentration-dependently and significantly enhanced the relaxation to GSNO (from 30±9% to 53±7%, control vs ascorbate 3 μM, n=9) and that to CysNO (from 28±6% to 45±3% control vs ascorbate 1 μM, n=7). Ascorbate alone did not affect the contraction to prostaglandin $F_{2\alpha}$. However, when 1 μM ascorbate was added 1 minute after 0.1 μM GSNO, it induced a rapid and transient relaxation of 90±2% (n=5). This relaxation was inhibited to 20±2% (n=5) by the superoxide generator pyrogallol (2 μM) which inhibits relaxations to NO in the rat gastric fundus (De Man et al., 1997). Ascorbate (1-3 μM) did not affect the relaxations to 0,01 μM NO (from 30±5% to 31±3%, control vs ascorbate 3 μM, n=6) or to nitrergic stimulation (1 Hz, 1ms pulse duration, 10s pulse trains; from 38±5% to 40±5%, control vs ascorbate 3 μM, n=6). As endogenous superoxide dismutase (SOD) protects the nitrergic neurotransmitter from breakdown (Martin et al., 1994), we reexamined the effect of ascorbate on nitrergic NANC relaxations after inhibition of SOD with diethyl dithiocarbamate (DETC). However, also after treatment of the muscle strips with DETC (1 mM), ascorbate (1-3 μM) had no effect on the relaxations to nitrergic stimulation (1 Hz; from 43±6% to 47±6%, control vs ascorbate 3 μM plus DETC, n=7).

These results show that relaxations to NO and to nitrergic stimulation of the rat gastric fundus are not influenced by ascorbate whereas relaxations to S-nitrosothiols are enhanced. Our results suggest that ascorbate decomposes S-nitrosothiols by inducing a rapid release of NO from the S-nitrosothiol. As ascorbate did not affect the relaxations to nitrergic stimulation it is concluded that S-nitrosothiols do not mediate nitrergic neurotransmission in the rat gastric fundus.

Lilley, E. & Gibson, A. (1996) *Br. J. Pharmacol.*, 119, 432-438.

Martin W., McAllister, K.H.M. & Paisley, K. (1994) *Neuropharmacology*, 33, 1293-1301.

De Man, J.G., De Winter B.Y., Boeckxstaens, G.E. *et al.*, (1997) *Br. J. Pharmacol.*, 119, 990-996.

117P A COMPARISON OF THE EFFECTS OF NITRIC OXIDE SYNTHASE INHIBITORS ON NON-ADRENERGIC, NON-CHOLINERGIC (NANC) RELAXATIONS OF THE RAT FUNDUS AND FROG OESOPHAGUS

S. J. Williams[1] & M. E. Parsons. Biosciences Division, University of Hertfordshire, College Lane, Hatfield, Herts. AL10 9AB.

We have previously shown that the nitric oxide synthase (NOS) inhibitor N^G-nitro-L-arginine (L-NOARG) can markedly reduce or abolish electrically evoked NANC relaxations of the rat fundus and frog oesophageal body in vitro suggesting an important role for nitric oxide in these responses (Williams & Parsons 1995, 1997). In the present study we have extended these observations to examine the specific neuronal NOS inhibitor 7-NINA (7-nitroindazole sodium salt) (Nakane *et al*, 1995) and the inducible NOS inhibitor AMT (2-amino-5,6-dihydro-methylthiazine) (Allawi *et al*, 1994).

Longitudinal muscle strips 2-3mm wide and 20mm long were prepared from the fundus of starved Charles River Wistar rats of either sex, weighing 250-350g. The tissues were mounted in 25ml organ baths containing modified Krebs-Ringer solution. Circular strips (c.2mm wide) from the oesophageal body of the frog (*Rana temporaria)* of either sex, weighing 14-25g, were mounted longitudinally in a 15ml organ bath containing Tyrodes solution. Tissues were placed between ring electrodes under a tension of 1g and responses were measured using isometric transducers. The bathing solutions contained indomethacin and guanethidine (10^{-6}M). The baths were maintained at 37°C, or room temperature for the frog, and aerated with 95% O_2 and 5% CO_2. In the presence of a maximal carbachol induced contraction (10^{-5}M), electrical field stimulation (1-10Hz, 2ms, 30V, 10s every 5min for the frog and 1-16Hz, 0.5ms, 40V, 10s every 5min for the rat) produced frequency dependent relaxations.

7-NINA at 10^{-5}M and 10^{-4}M had no effect on NANC relaxations in the rat fundus (n=6) and produced a slight (29.52 ± 3.4%, 10^{-4}M at 4Hz) but significant (P<0.05) potentiation of the response in the frog oesophagus (n=6) but the latter was not reversed by incubation with L-arginine ($5x10^{-3}$M).

AMT (10^{-6}M-10^{-4}M) produced a significant (68.33 ± 8.86% with 10^{-5}M at 4Hz, P<0.01, n=6) but non-concentration related inhibition of the relaxant responses in the rat fundus. In the frog oesophagus AMT produced a significant potentiation at 10^{-6}M (P<0.05, n=6) but a significant inhibition at 10^{-5}M (42.19 ± 10.84 at 4Hz, P<0.01, n=6) and at 10^{-4}M abolished the response (n=6). None of these effects were reversed by L-arginine.

These data confirm that 7-NINA has no effect on peripheral NO mediated responses. The AMT data is difficult to explain but the lack of significant reversibility with L-arginine suggests that its effect does not involve inhibition of inducible NOS.

Allawi, H.S., Wallace, P., Pitcher, A. *et al.* (1994). *Br. J. Pharmacol.*, 113, 282-286.
Nakane, M., Klinghofer, V., Kuk, J.E. *et al.* (1995) *Mol. Pharmacol.*, 47, 831-834
Williams, S.J. & Parsons, M.E. (1995) *Br. J. Pharmacol,. 116*, 1789-1796.
Williams, S.J. & Parsons, M.E. (1997) *Br. J. Pharmacol,.*112, 179-185.

118P INHIBITION OF NITRERGIC NEUROTRANSMISSION BY OXIDANT STRESS: EFFECTS OF SUPEROXIDE DISMUTASE MIMETICS

W. Martin, J.S.L. Mok & K. Paisley, Clinical Research Initiative, West Medical Building, University of Glasgow, Glasgow, G12 8QQ.

Interest is growing in the potential development of low molecular weight, membrane-permeant superoxide dismutase (SOD) mimetics as therapeutic agents in pathologies associated with oxidant stress. The aim of this study was to determine if putative SOD mimetics possessed the ability of authentic SOD to reverse the blockade of nitrergic neurotransmission produced in the bovine retractor penis (BRP) muscle following inhibition of endogenous Cu-Zn SOD and generation of superoxide anion (Martin *et al.*, 1994).

Superoxide dismutase activity of authentic SOD and the SOD mimetics was assessed by their ability to inhibit the superoxide-catalysed reduction of nitro blue tetrazolium (NBT; Martin & Mok, 1997). BRP muscle strips were mounted for isometric tension recording within Ag/AgCl ring electrodes. Adrenergic motor responses were blocked and the tone raised using guanethidine (30 μM). Nitrergic relaxation was evoked by field stimulation (4 Hz, 10 s) with a pulse width of 0.5 ms at supramaximal voltage. Endogenous Cu-Zn SOD was inactivated by incubating BRP strips for 120 min with diethyldithiocarbamate (DETCA; 3 mM). LY 83583 (1 μM) was used to generate superoxide anion. The SOD mimetic compounds investigated were 4-hydoxy 2,2,6,6-tetramethylpiperidine-1-oxyl (tempol), 4-phenyl-2,2,5,5-tetramethyl-3-imidazolin-1-yloxy-3-oxide (PTIYO), 4,5-dihydroxy-1,3-benzene disulfonic acid (tiron), manganese (III) tetrakis (1-methyl-4-pyridyl) porphyrin pentachloride (MnTMPyP) and manganese (III) tetrakis (4-benzoic acid) porphyrin (MnTBAP).

Data are expressed as mean ± s.e. mean of ≥ 5 observations and differences were determined by ANOVA followed by the Bonferroni post-test.

Each of the SOD mimetics inhibited superoxide-catalysed reduction of NBT (pEC_{50} values): MnTMPyP (7.86 ± 0.04), MnTBAP (6.04 ± 0.04), tempol (4.29 ± 0.02), tiron (4.28 ± 0.19), and PTIYO (3.92 ± 0.03). The pEC_{50} for SOD was 0.07 ± 0.04 U ml^{-1}. Nitrergic nerve stimulation evoked relaxations of 96.8 ± 1.5 %. These relaxations were reduced to 3.9 ± 3.0 % (P<0.001) following addition of LY 83583 to DETCA-treated tissues. Treatment with SOD produced a concentration-dependent reversal of this blockade (maximum relaxation 46.9 ± 6.4 %, P<0.001, pEC_{50} 0.66 ± 0.09 U ml^{-1}). MnTMPyP produced a similar reversal of blockade (maximum relaxation 57.1 ± 10.7 %, P<0.001, pEC_{50} 4.23 ± 0.66). In contrast, even at the highest concentrations tested, MnTBAP (0.1 mM), tempol (1 mM), tiron (1 mM) and PTIYO (0.1 mM) each failed to produced a significant reversal of blockade.

In conclusion, MnTMPyP had strikingly greater SOD-like activity than any of the other SOD mimetics in the NBT assay. Furthermore, this was the only SOD mimetic to possess the ability of SOD to reverse the blockade of nitrergic neurotransmission produced by an oxidant stress. This compound may thus provide a lead in the development of SOD mimetics as therapeutic agents in the treatment of neuropathies associated with oxidant stress.

Martin, W., McAllister, K.H.M. & Paisley, K. (1994). *Neuropharmacol.*,33, 1293-1301.
Martin, W. & Mok, J.S.L. (1997). Edinburgh BPS meeting.

119P 5-HT$_4$-RECEPTOR-MEDIATED RESPONSES IN NORMAL AND HYPERREFLEXIC HUMAN BLADDER

S.W. Martin[1], C.R.Chapple,[1]R.Chess-Williams[2]
[1]Department of Urology, Royal Hallamshire Hospital, Sheffield, U.K. [2] Department of Biomedical Science, University of Sheffield, U.K.

In human isolated detrusor muscle, 5-HT facilitates neuromuscular cholinergic transmission by acting on pre-junctional 5-HT4 receptors. (Tonnini *et al.*, 1994; Candura *et al.*, 1996). In this study, the effects of 5-HT on facilitation of responses to electrically-field stimulation (EFS) were compared in isolated strips of normal and hyperreflexic human bladder.

Normal bladder was obtained from patients undergoing cystectomy for bladder cancer. Hyperreflexic bladder was obtained from patients undergoing clam ileocystoplasty. Full informed consent was acquired. Strips of detrusor muscle were mounted under 1g resting tension in organ baths (containing gassed Krebs solution at 37°C) for isometric tension measurements. Methiothepin (1μM), ketanserin (1μM) and ondansetron (1μM) were present throughout the experiment to block 5-HT1, 5-HT2 and 5-HT3 receptors respectively. Following a 60-minute equilibration period, responses to 100mM KCl were obtained. The tissues were then field-stimulated (10Hz, 0.1msec duration, 60V) at 100sec intervals until consistent responses were obtained. In an initial series of experiments, 5HT was then administered cumulatively in half-log increments. Cumulative concentration-response curves to 5-HT and cisapride were then obtained.

5-HT produced concentration-related increases in the contractile responses to EFS in both normal and hyperreflexic bladder. EC50 values were not significantly different (p= 0.43). The maximum potentiation induced by 5-HT in hyperreflexic detrusor muscle was significantly (p=0.018) reduced compared to normal detrusor muscle (Table1).

Cisapride also produced concentration-related enhancement of field-stimulated responses. The drug acted as a partial agonist relative to 5-HT. As with 5-HT, the maximum potentiation due to cisapride was depressed in hyperreflexic detrusor muscle but in this case, the difference was significant only when the data was expressed as a percentage of the resting response to EFS (Table1).

Table 1: 5HT and cisapride EC50 and maximum response data:

	NORMAL DETRUSOR	HYPERREFLEXIC DETRUSOR
5HT		
EC50 (nM)	25.1(14.0-44.9)	39.1(14.5-105.2)
Max. (grams)	0.58 ± 0.07	0.28 ± 0.09*
Max (% 100mM KCl)	25.4 ± 3.1	11.4 ± 3.8 *
Max % Resting EFS	85.4 ±15.1	40.3 ± 12.1*
n	9	7
CISAPRIDE		
EC50 (μM)	0.28(0.11-0.71)	0.66(0.18-2.41)
Max (grams)	0.11 ± 0.06	0.09 ± 0.06
Max (% 100mM KCl)	6.45 ± 1.65	6.40 ± 3.62
Max (%Resting EFS)	31.2 ± 4.3	15.4 ± 4.7 *
Max (% 5HT Max)	30.6 ± 6.8	43.1 ± 5.2
n	4	4

* $p \leq 0.05$, Student t-test.

We conclude that that the response to 5-HT4 receptor stimulation is depressed in hyperreflexic human bladder.

Candura, S.M., Messori, E., Franceschetti, G.P. *et al.* (1996) Br. J. Pharmacol., **118**, 1965-1970.
Tonnini, M., Messori, E., Franceschetti, G.P. *et al* . (1994) Br. J. Pharmacol., **113**, 1-2.

120P OBJECTIONS TO CLASSICAL MODELS OF PHARMACOLOGICAL AGONISM

E. Agneter[1], E.A. Singer[1], T.J. Feuerstein[2], W. Sauermann[3] [1]Institute of Pharmacology, University of Vienna, Währinger Str. 13a, 1090 Vienna, Austria; [2]Sektion Klinische Neuropharmakologie der Neurologischen Universitätsklinik, Neurozentrum, D-79106 Freiburg, and [3]DATAMAP, Munzinger Str. 5A, D-79111 Freiburg, Germany

Agonist dissociation constants (K_A's) may be estimated according to Furchgott (1966) or to Black and Leff (1983). Both models do not include the possibility that the relative effect, E/E_{max}, may be proportional to fractional receptor occupation by an agonist at concentration [A], i.e. to $[A]/(K_A + [A])$. Since this direct proportionality is *a priori* excluded, these methods may detect spare receptors even if there are non. (E.g. please compare the results of Agneter et al. (1993) with Agneter et al. (1997)).

With respect to Black and Leff, the reason is the following: In their operational model, $E/E_{max} = \tau[A]/(K_A + (1 + \tau)[A])$, the ratio $\tau/(1 + \tau)$ is always < 1 ($\tau = R_o/K_E$, R_o: total receptor concentration, K_E: concentration of the agonist-receptor complex, [AR], for half the maximum possible effect. When concentration-response data, reflecting direct proportionality, are fitted with the Black and Leff model misleading results are obtained, e.g.: for values E/E_{max} near 1 the only possibility for the operational model to cope with this situation is to estimate τ as very large since only for large τ the ratio $\tau/(1 + \tau) \approx 1$. For large τ, the operational model can be written approximately as $E/E_{max} = [A]/(K_A/(1 + \tau) + [A])$. Then, the half maximal effect would occur for $[A] = K_A/(1 + \tau)$, and therefore K_A would be overestimated by the large factor $(1 + \tau)$. For small τ, [AR] can assume only small values. Therefore, the mathematical form of the "transducer function", $E/E_{max} = [AR]/(K_E + [AR])$, is quite irrelevant: If the transducer function is used only for small arguments [AR] this function is approximately linear and solely depends on K_E. Then $E/E_{max} \approx [AR]/K_E$ since $f(x) \approx f'(0) \cdot x$ for x close to zero, corresponding to $E/E_{max} \approx \tau\,[A]/(K_A + [A])$. Thus, for large [A], $E/E_{max} \approx \tau$. This is an obvious inconsistency. When there is no direct proportionality between relative effect and fractional receptor occupation, response as a function of the agonist concentration is no longer a symmetric sigmoid in the (usual) semi-logarithmic scale (Feuerstein et al. 1994). The operational model does not allow for such a shape and therefore an estimate of a receptor reserve is biased.

When appropriate dose-response-curves of α_2-autoreceptor mediated inhibition of electrically evoked [^{3}H]-noradrenaline release in the rat cortex were used to estimate a receptor reserve, receptor reserves of 92% and 83% according to the methods of Black and Leff and Furchgott, respectively were estimated. However a mixture of noradrenaline and yohimbine designed to activate 75% of the α_2-receptors did not obtain the maximum effect seen with noradrenaline alone. With our model of receptor agonism the receptor reserve for α_2-autorecptors in rat cortex was estimated to be zero. This is in line with the results obtained with the mixture of noradrenaline and yohimbine.

To quantify spare receptors, mathematical models with a potentially asymmetric function should be used, developed on the basis of occupation of individual receptors on individual functional units (Feuerstein et al. 1994). Evaluation methods, like those of Furchgott (1966) or of Black and Leff (1983), which neglect potentially asymmetric curves do not seem appropriate to quantify spare receptors. These methods may detect spare receptors where they do not exist (Agneter et al., 1997).

Agneter E., Drobny H., and Singer E.A. (1993) *British J Pharmacology* 108: 370-375.

Agneter E., Singer EA., Sauermann W. et al. (1997) *Naunyn-Schmiedeberg's Arch Pharmacol* 356: 283-292

Black JW. and Leff P. (1983) *Proc R Soc B* 220:141-162

Feuerstein TJ., Sauermann W., Allgaier C., et al. (1994) *Naunyn-Schmiedeberg's Arch Pharmacol* 350:1-9

Furchgott RF. (1966) *Adv Drug Res* 3:21-55

121P MODULATION OF NEURALLY-EVOKED CHOLINERGIC CONTRACTIONS OF THE GUINEA-PIG ILEUM BY ENDOGENOUS ADENOSINE

J. J. Lee & M. E. Parsons. Biosciences Division, University of Hertfordshire, College Lane, Hatfield, Herts. AL10 9AB.

We have previously shown that adenosine, acting at presynaptic adenosine A_1-receptors, can suppress cholinergic nerve-mediated contractions of the guinea-pig ileum in response to electrical field stimulation (EFS) (Lee & Parsons, 1996). The present study extends this observation and examines a possible role for endogenous adenosine in modulating cholinergic nerve function.

Segments of distal ileum, 2cm in length, were obtained from Dunkin-Hartley guinea-pigs (600-800g) of either sex and mounted under a tension of 1g in 25ml organ baths containing Krebs solution at 37°C and aerated with 95%O_2/5%CO_2. Tissues were continuously stimulated coaxially by EFS (10V, 5ms, 0.1Hz) with parallel platinum electrodes delivered from a Grass stimulator. Isometric contractions were measured by a force transducer. All experiments were repeated on tissues from no less than 5 animals.

Adenosine (0.2-28μM) and the selective A_1-receptor agonist 2-chloroadenosine (5-160nM), inhibited EFS evoked contractions (EC_{50}s = 2.12 ±0.39μM, and 28.0 ±1.4nM, respectively). The effect was antagonised by 20nM DPCPX (1,3-dipropyl-8-cyclopentylxanthine), a specific A_1-receptor antagonist (Lohse *et al*, 1987), with an approximate dose-ratio of 3 for adenosine and 10 for 2-chloroadenosine. The adenosine uptake inhibitors dipyridamole (20nM) and S-(4-nitrobenzyl)-6-thioinosine (NBTI) (3nM) caused respectively, an approximate 4 fold and 2 fold increase in the inhibitory effect of 1.6μM adenosine. In contrast, inhibition induced by 50nM 2-chloroadenosine, which is not a substrate for the uptake process (Daly, 1983), was not altered in the presence of the uptake blockers.

The uptake inhibitors themselves, when applied at higher concentrations, produced a significant reduction of evoked contractions. Thus, a 62.0 ±3.5% and 69.4 ±6.4% reduction was observed following application of 1μM dipyridamole and 300nM NBTI, respectively. In both cases, the effect could be sustained for up to 30 minutes and reversed by DPCPX (20nM) to 88.6 ±3.1% (for dipyridamole) and 94.4 ±5.6% (for NBTI) of the original contraction magnitude. DPCPX (20nM) alone produced a small (10.8 ±2.4%) but significant potentiation of the twitch height.

The data confirm the existence of inhibitory presynaptic adenosine A_1-receptors modulating cholinergic nerve function in the guinea-pig ileum and suggests that these receptors can be activated by endogenous adenosine released as either adenosine itself or ATP during EFS.

Daly, J.W. (1983) in *Physiology and Pharmacology of Adenosine Derivatives.*, ed. Daly, J.W., Kuroda, Y., Phillis, J.W. *et al* pp. 275-291. New York: Raven Press.

Lee, J.J. & Parsons, M.E. (1996). *Br. J. Pharmacol.*, **119**, 199P.

Lohse, M.J., Klotz, K.N., Lindenborn-Fotinos, J. *et al*, (1987). *Naunyn-Schmiedeberg's Arch. Pharmacol.*, **336**, 204-210.

122P CHOLINESTERASE ACTIVITY IN HUMAN ISOLATED AIRWAYS

X. Norel, L. Walch, B. Leconte, J.P. Gascard & C. Brink, CNRS-ERS 566, CCML, 92350 Le Plessis-Robinson, France.

Airway muscle contraction induced by endogenous acetylcholine depends on the hydrolysis of this neurotransmitter by the cholinesterases (ChE) (Norel *et al.*, 1993). The aim of this study was to determine biochemical characteristics of these enzymes in the human bronchus. The enzymatic activities of the ChE were measured by the Ellman's colorimetric method. Measurements were made in bronchial homogenates and in bath fluids where bronchial rings (intact or without epithelium) were incubated for 1h in Tyrode's solution (37°C; gassed with CO_2/O_2). These samples were submitted to osmotic shock. Acetylcholinesterase (AChE; EC 3.1.1.7) and butyrylcholinesterase (BChE; EC 3.1.1.8) activities were measured in presence or absence of selective inhibitors (BW284C51: 1 μM and iso-OMPA: 10 μM (Massoulié *et al.*, 1993)). Results are means±SEM derived from 4 lung samples.

The kinetic parameters of the ChE were determined in homogenates and results are presented in table:

Bronchial homogenate		
AChE	**BChE**	
Vmax	*Vmax*	*Vss*
7.74±0.80	2.95±0.68	8.57±1.76
Km	*Km*	*Kss*
153±16	51±13	1179±320

The enzymatic kinetic parameters (Vmax, Vss) are expressed in mIU/mg protein and (Km, Kss) in μM.

ChE activity measured in bath fluid samples of bronchial rings are shown in figure:

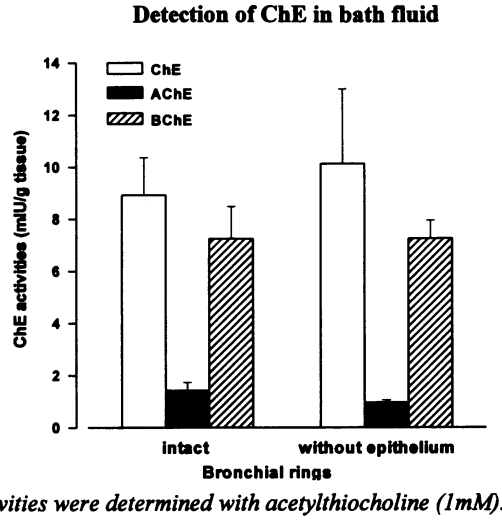

ChE activities were determined with acetylthiocholine (1mM).

ChE activities are present in human airways, in agreement with a previous report (Norel *et al.*, 1993). A soluble isoform of BChE was released by bronchial rings independently of the epithelial layer.

Massoulié *et al.* (1993) *Prog. Neurobiol.* 41, 31-91.
Norel *et al.* (1993) *Br. J. Pharmacol.* 108, 914-919.

123P BEYOND THE SCHILD PLOT: A NONLINEAR MODEL OF THE SIMULTANEOUS EVALUATION OF SURMOUNTABLE AND INSURMOUNTABLE ANTAGONISM

Frank A.M. Peeters, VIRCO, Drie Eikenstraat 661, 2650 Edegem, Belgium

The Schild plot and the method of Van Rossum have been used for decades to evaluate the activity of surmountable antagonists in pharmacological experiments (Arunlakshana & Schild, 1959; Van Rossum, 1963). However these methods have some serious drawbacks : the control agonist concentration-effect curve (CEC) is over-weighed; CECs that are positioned left from the control curve cannot be used and the methods are not valid if unsurmountable antagonism is observed (i.e. when the Schild slope differs from unity). Recently, Lew & Angus (1995) developed a nonlinear model that estimates the pKb for surmountable antagonism directly from the agonist EC50 values. In this method all agonist curves are equally weighed and curves left from the control curve can be included in the analysis. However all the individual EC50 values need to be calculated before they can be inputted in the model. We have extended the model of Lew & Angus in order to avoid this tedious calculation of the agonist EC50 values. In addition, we have added a correction for unsurmountable antagonism based on the pD2' method of Van Rossum (1963).

In our new model, the agonist CECs are directly fitted to a logistic equation of the form : $E = Emax / (1 + (EC50/[A])^n)$ in which [A] is the agonist concentration and E the response. This equation is further corrected for the effect of the antagonist [B], and we hereby assume that the slope (n) of the agonist curve is unaltered by the antagonist :

$$E = \left(Emax / \frac{[B]+10^{-pD2'}}{10^{-pD2'}}\right) / \left(1 + \left(\frac{EC50}{[A]} \frac{[B]+10^{-pKb}}{10^{-pKb}}\right)^n\right)$$

The estimated parameters are the EC50, maximal response (Emax) and the slope (n) of the agonist control CEC, and the parameters describing the surmountable (pKb) and unsurmountable (pD2') portion of the inhibition provoked by the antagonist.

Table 1 table shows the results of a typical experiment. It depicts the effect of a serotonin S_2 antagonist on the contractions induced by serotonin in the rat aorta (8 concentrations per agonist CEC; control CEC + 3 antagonist concentrations; 6-8 replicates).

Method	pKb		Error type
Van Rossum	5.93 ± 0.09		SD
Schild plot	5.89 ± 0.17	slope = -1.03	SE
Lew & Angus	5.92 ± 0.04		ASE
New model	5.88 ± 0.05	pD2' = 4.10 ± 0.09	ASE
1000 bootstraps	5.87 ± 0.04	pD2' = 4.11 ± 0.08	SD

SD=Stand. deviat. SE=Stand. Error ASE=Asymptotic Stand. Error

The new model adequately determines the pKb value of the antagonist, and detects an unsurmountable effect at higher antagonist concentrations. It uses all the available data in a one-shot nonlinear regression, and it can therefore even integrate incomplete agonist CECs. The results are independent of the software package that was used (SAS, Tablecurve 3D, Sigmaplot or Fortran Powerstation IMSL routines). Further, the ASE values estimated by the nonlinear regression programs seem to give a good estimate of the true error, as shown from bootstrapping experiments. In this methodology, the replicate CEC curves were randomly replaced to generate noisy data. This procedure was repeated 1000 times and the mean and SD of all the estimated parameters were calculated.

We conclude that the model presented here provides an easy and more correct approach than the Schild plot or the method of Van Rossum.

Arunlakshana O. & Schild H.O. (1959) *Br. J. Pharmacol.* 14, 48-58.
Lew M.J. & Angus J.A. (1995) *TIPS* 16, 328-337.
Van Rossum J.M. (1963) *Arch. Int. Pharmacodyn.* 143, 299-330.

124P FREQUENCY-DEPENDENT AND α_2-ADRENOCEPTOR-REGULATED FACILITATION OF EVOKED NORADRENALINE OVERFLOW BY ENDOGENOUS ATP THROUGH PREJUNCTIONAL P_{2Y}-PURINOCEPTORS

J. Smit, E.J.J. van Tintelen, I.F. Palm, F. Brouwer and J. Zaagsma. Department of Molecular Pharmacology, University of Groningen, A. Deusinglaan 1, NL-9713 AV Groningen, The Netherlands

Noradrenaline (NA) and ATP are co-transmitters in many postganglionic sympathetic nerves. ATP (and its metabolites) may exert a variety of prejunctional and postjunctional effects by acting on purinoceptors. Prejunctionally, the P_{2Y}-purinoceptor subtype has been claimed to possess inhibitory as well as facilitatory properties on sympathetic neurotransmission in various organ systems (Von Kügelgen *et al.*, 1994; Sperlach and Vizi, 1991).

In the present study the effects of Reactive Blue 2 (RB2), known to be P_{2Y}-selective at low micromolar concentrations (Kennedy, 1990), were investigated on basal and electrically evoked endogenous noradrenaline (NA) overflow in the portal vein as well as on mean arterial pressure (MAP) and heart rate (HR) in freely moving Wistar rats, both in the absence and presence of α_2-adrenoceptor blockade with yohimbine (0.5 mg kg^{-1}) (YOH). At least one week prior to commencing the experiments, the animals were provided with a sample cannula in the portal vein and a bipolar stimulation electrode around it; a second cannula was implanted in the abdominal aorta for monitoring blood pressure and HR and for injection of drugs. To induce NA overflow, the portal vein nervous plexus was stimulated by biphasic block pulses (5 mA; 3 ms) at low (2Hz) and high (15Hz) frequencies. Portal plasma NA concentration was determined by HPLC-ECD.

At 2Hz, RB2 (0.003-1.0 μmol kg^{-1}) dose-dependently inhibited evoked NA overflow, with a maximum inhibition of 52 ± 8% ($p < 0.01$) of control being reached already with 0.1 μmol kg^{-1}. However, at 15Hz, which produced NA overflow that was 4.4-fold higher than at 2Hz, RB2 was totally inactive, even at the highest dose. At 2Hz and 15Hz YOH increased evoked NA overflow similarly to 292 ± 17% ($p < 0.001$) and 318 ± 35% ($p < 0.001$) of control, respectively. Remarkably, in the presence of YOH, RB2 dose-dependently diminished the YOH-potentiated NA overflow at 2Hz and 15Hz with a similar potency, with a maximum inhibition of 49 ± 7% and 54% ± 11% at 1.0 and 0.1 μmol kg^{-1}, respectively. Basal NA, MAP and HR were not influenced by RB2 at all. YOH increased basal NA overflow from 272 ± 21 to 571 ± 59 pg ml^{-1} ($p < 0.001$) and HR by 49 ± 10 beats min^{-1} ($p < 0.001$) but these effects were not influenced by RB2 either, although basal NA overflow tended to be lower at all RB2 doses.

The results clearly indicate that during local electrical stimulation of the portal vein of the freely moving rat, endogenous overflow of NA is under marked facilitatory control of its co-transmitter ATP through prejunctional P_{2Y}-receptors, and that this facilitation is inversely related to prejunctional α_2-adrenoceptor autoregulation.

Kennedy, C. (1990) Arch. Int. Pharmacodyn. Ther. 303, 30-50
Sperlagh, B. and Vizi, E.S. (1991) J. Neurochem. 56, 1466-1470
Von Kügelgen, I. *et al.* (1994) Fundam. Clin. Pharmacol. 8, 207-213